Intracellular pH Modulates Taste Receptor Cell Volume and the Phasic Part of the Chorda Tympani Response to Acids

Vijay Lyall,[1] Hampton Pasley,[1] Tam-Hao T. Phan,[1] Shobha Mummalaneni,[1] Gerard L. Heck,[1] Anna K. Vinnikova,[2] and John A. DeSimone[1]

[1]Department of Physiology and [2]Department of Internal Medicine, Virginia Commonwealth University, Richmond, VA 23298

The relationship between cell volume and the neural response to acidic stimuli was investigated by simultaneous measurements of intracellular pH (pH_i) and cell volume in polarized fungiform taste receptor cells (TRCs) using 2',7'-bis-(2-carboxyethyl)-5-(and-6)-carboxyfluorescein (BCECF) in vitro and by rat chorda tympani (CT) nerve recordings in vivo. CT responses to HCl and CO_2 were recorded in the presence of 1 M mannitol and specific probes for filamentous (F) actin (phalloidin) and monomeric (G) actin (cytochalasin B) under lingual voltage clamp. Acidic stimuli reversibly decrease TRC pH_i and cell volume. In isolated TRCs F-actin and G-actin were labeled with rhodamine phalloidin and bovine pancreatic deoxyribonuclease-1 conjugated with Alexa Fluor 488, respectively. A decrease in pH_i shifted the equilibrium from F-actin to G-actin. Treatment with phalloidin or cytochalasin B attenuated the magnitude of the pH_i-induced decrease in TRC volume. The phasic part of the CT response to HCl or CO_2 was significantly decreased by preshrinking TRCs with hypertonic mannitol and lingual application of 1.2 mM phalloidin or 20 μM cytochalasin B with no effect on the tonic part of the CT response. In TRCs first treated with cytochalasin B, the decrease in the magnitude of the phasic response to acidic stimuli was reversed by phalloidin treatment. The pH_i-induced decrease in TRC volume induced a flufenamic acid–sensitive nonselective basolateral cation conductance. Channel activity was enhanced at positive lingual clamp voltages. Lingual application of flufenamic acid decreased the magnitude of the phasic part of the CT response to HCl and CO_2. Flufenamic acid and hypertonic mannitol were additive in inhibiting the phasic response. We conclude that a decrease in pH_i induces TRC shrinkage through its effect on the actin cytoskeleton and activates a flufenamic acid–sensitive basolateral cation conductance that is involved in eliciting the phasic part of the CT response to acidic stimuli.

INTRODUCTION

Sour taste is a primary taste modality and is uniquely associated with acidic stimuli. It evokes an innate rejection response to extremely acidic or sour stimuli, limiting the ad libitum ingestion of acid (Beauchamp et al., 1991; Scott and Plata-Salaman, 1991). In this regard, along with the lungs and kidneys, which are the primary organs for acid secretion, acid sensing taste receptor cells (TRCs) in the oral cavity, by restricting the intake of acid, function as part of a multi-organ system to maintain acid–base homeostasis. Acids in aqueous solution yield H^+, which can alter both the extracellular (pH_o) and intracellular pH (pH_i) of cells. A large number of enzymatic reactions, channels, transporters, and intracellular signaling events are modulated by changes in pH_i. It is, therefore, a special challenge to identify the specific channels, transporters, and other intracellular signaling events in TRCs that sustain acid taste transduction and ultimately the cortical events resulting in sour taste sensation. In spite of this complexity, some progress has been made in understanding the underlying mechanisms involved in sour taste transduction at the level of TRCs.

Recent studies indicate that the proximate signal for sour taste transduction is an acid-induced decrease in pH_i in a subset of TRCs (Lyall et al., 2001). In the case of strong acids, an apical adenosine 3'5'-cyclic monophosphate (cAMP)–sensitive, but Ca^{2+}-insensitive H^+ conductance allows H^+ entry and the subsequent decrease in TRC pH_i (Lyall et al., 2002a; 2004a). However, H^+-gated channels, such as the acid sensing ion channel (ASIC) in the apical membrane and both ASIC (Ugawa et al., 1998; Lin et al., 2002) and hyperpolarization-activated channels (HCN) (Stevens et al., 2001) in the basolateral membrane of TRCs, and TASK-2, a two pore domain K^+ channel (Lin et al., 2004; Richter et al., 2004a) may also play a role in sour taste transduc-

Correspondence to Vijay Lyall: vlyall@hsc.vcu.edu

The Journal of General Physiology

tion. These channels in the basolateral membrane could be activated if H^+ can cross tight junctions and decrease pH in the basolateral compartment. However, recent studies suggest that in mice ASIC2 is not required for acid taste (Richter et al., 2004b). In contrast, weak organic acids do not seem to have apical membrane receptors. They enter TRCs across the apical membrane by passive diffusion as lipid soluble undissociated neutral molecules. Once inside the cell they dissociate to generate H^+ and decrease TRC pH_i (Lyall et al., 2001). TRCs also contain 5-nitro-2-(3-phenylpropylamino)-benzoate (NPPB)-sensitive stretch-activated Cl^- channels (Gilbertson, 2002). The presence of an NPPB-sensitive Cl^- channel activated by acid was demonstrated in mouse taste cells (Miyamoto et al., 1998). These results suggest a role for Cl^- channels in acid taste transduction. In addition to Cl^- channels, there is also evidence that NPPB-insensitive poorly selective cationic conductance in the apical receptive membranes of mouse TRCs may also be involved in sour taste transduction (Miyamoto et al., 1998). The above data suggest that sour taste transduction is mediated via multiple pathways. Similarly, in the case of other acid-sensitive cells, such as the central chemosensitive neurons, a multiple factors model has been proposed for acid signaling (Putnam et al., 2004).

Recent studies in our laboratory have focused on identifying specific cellular mechanisms that determine the neural response profiles to acidic stimuli. Similar to other taste stimuli, acidic stimuli elicit chorda tympani (CT) responses that are composed of two components with distinct temporal characteristics: a rapid transient increase in the phasic neural response that slowly declines to a quasi-steady state, defined as the tonic phase of the neural response. Treating rat tongue with specific membrane-permeable blockers of carbonic anhydrases (MK-417 or MK-507) inhibited both the phasic and tonic components of the CT response to CO_2 (Lyall et al., 2001, 2002b). This indicates that an acid-induced decrease in TRC pH_i is necessary to elicit both the phasic and the tonic components of the CT response to acid stimulation. In a subset of TRCs a decrease in pH_i is followed by an increase in intracellular Ca^{2+} ($[Ca^{2+}]_i$) (Liu and Simon, 2001; Lyall et al., 2003; Richter et al., 2003). An increase in TRC $[Ca^{2+}]_i$ activates basolateral Na^+-H^+-exchanger-1 (NHE-1) and results in neural adaptation to both strong and weak acid stimuli (Lyall et al., 2002a, 2004a). Neural adaptation is related to the tonic part of the CT response to acidic stimuli. Therefore, a primary decrease in TRC pH_i, followed by a secondary increase in $[Ca^{2+}]_i$, and the subsequent activation of basolateral NHE-1 are specific events related to the tonic part of the neural response only. However, at present a major unsolved problem in acid taste transduction is: how is the decrease in pH_i related to the phasic part of the neural response to acid stimulation?

In this study, we tested the hypothesis that a decrease in pH_i induces a decrease in TRC volume by altering the cell actin cytoskeleton leading to the activation of one or more membrane conductances that are involved in eliciting the phasic part of the CT response to acidic stimuli. This hypothesis is based on our previous studies in which hypertonic solutions of mannitol or cellobiose (Lyall et al., 1999) or ethanol (Lyall et al., 2005a,b) induced cell shrinkage and elicited a transient phasic CT response. This suggests that a decrease in cell volume is an intracellular signal for eliciting a transient neural response. Second, since only a transient phasic response was observed in ethanol solutions in the absence of permeable ions on the apical side, it would appear that cell depolarization involves changes in a basolateral membrane ion conductance or conductances uniquely associated with transient phasic responses (Lyall et al., 2005a,b). To test this hypothesis, we investigated the relationship between TRC volume and the CT response to acidic stimuli by simultaneously monitoring pH_i and cell volume in polarized rat fungiform TRCs loaded with 2',7'-bis-(2-carboxyethyl)-5-(and-6)-carboxyfluorescein (BCECF) using imaging techniques in vitro, and by rat CT taste nerve recordings in vivo. The results demonstrate that during acid taste transduction a decrease in TRC pH_i induces cell shrinkage through its effect on the cell actin cytoskeleton. A decrease in volume activates a flufenamic acid–sensitive nonselective cation conductance in the basolateral membrane of TRCs that is involved in eliciting the phasic part of the CT response to acidic stimuli. Some of the data have appeared in abstract form (DeSimone et al., 2005).

MATERIALS AND METHODS

In Vitro Studies

Simultaneous Measurement of TRC Volume and pH_i Using BCECF. The animals were housed in the Virginia Commonwealth University animal facility in accordance with institutional guidelines. All in vitro and in vivo animal protocols were approved by the Institutional Animal Care and Use Committee (IACUC) of Virginia Commonwealth University. Female Sprague-Dawley rats (150–200 g) were anesthetized by exposing them to the inhalation anesthetic, isoflurane (1.5 ml), in a desiccator. When rats were fully unconscious, a midline incision was made in the chest wall and the aorta severed. The tongues were then rapidly removed and stored in ice-cold Ringer's solution (R; Table I). The lingual epithelium was isolated by collagenase treatment. A small piece of the anterior lingual epithelium containing a single fungiform papilla was mounted in a special microscopy chamber as described earlier (Lyall et al., 2001).

Simultaneous measurement of cell volume changes and pH_i were made using the pH-sensitive dye BCECF and recording at both the pH-sensitive and pH-insensitive (isosbestic) wavelengths

TABLE I

Composition of Solutions Used in In Vitro Experiments

	R	C	NH$_4$Cl	NMDGCl	NMDGCl/NH$_4$Cl	HCl	CO$_2$/HCO$_3$$^{-}$[d]	HK[e]
	mM	*mM*	*mM*	*mM*	*mM*	*mM*	*mM*	*mM*
NaCl	140	150	135			150	78	4.6
KCl	5	5	5	5	5	5	5	140
CaCl$_2$	1	1	1	1	1	1	1	2
MgCl$_2$	1	1	1	1	1	1	1	1
NaPy[a]	10							
HEPES	10	10	10	10	10			10
Glucose	10	10	10	10	10	10	10	10
NMDGCl				150	135			
NH$_4$Cl[b]			15		15			
HCl[c]						1		
NaHCO$_3$							72	
pH	7.4	7.4	7.4	7.4	7.4	3.0	7.4	6.5–8.0

[a]NaPy, sodium pyruvate; R, Ringer's solution; C, control solution; NH$_4$Cl, solution containing NH$_4$Cl; NMDG-Cl, Na$^+$-free solution; NMDG/NH$_4$Cl, Na$^+$-free solution containing NH$_4$Cl; HCl, solution containing HCl.

[b]15 mM Na-acetate replaced 15 mM NH$_4$Cl.

[c]58.3 mM acetic acid was used instead of 1 mM HCl (pH 3.0); 50 mM KCl replaced 50 mM NaCl; Cl$^-$-free solution contained gluconate salts of Na$^+$, K$^+$, Ca^{2+}, and Mg^{2+}, and control solution was adjusted to pH 7.8 or 6.7.

[d]CO$_2$/HCO$_3$$^-$ solution was continuously bubbled with 10% CO$_2$.

[e]HK, high K$^+$ solutions containing 10 μM nigericin.

(Muallem et al., 1992). TRCs within the taste bud were loaded with BCECF. The detailed method for the measurement of TRC pH$_i$ using BCECF imaging has been described earlier (Lyall et al., 2001). Small regions of interest (ROIs) in the taste bud (diameter 2–3 μm) were chosen in which changes in the fluorescence intensity ratio (FIR; F$_{490}$/F$_{440}$) were analyzed using imaging software (TILLvisIon v 4.0.7.2; TILL Photonics). Each ROI contained two to three receptor cells. Thus the fluorescence intensity recorded for an ROI represents the mean value from two to three receptor cells within the ROI. In a typical experiment, the FIR measurements were made in an optical plane in the taste bud containing at least four ROIs (~8–12 cells). The background and autofluorescence at 490 and 440 nm were corrected from images of a taste bud without the dye. The changes in TRC pH$_i$ were calibrated by bilateral perfusion of high K$^+$ solutions (HK; Table I) containing 10 μM nigericin adjusted to pH values between 6.5 and 8.0. The relative changes in TRC volume were monitored at the isosbestic wavelength 440 nm. The fluorescence intensity at this wavelength is independent of pH and reflects the dye concentration inside the cell. Dye loss and bleaching was significantly reduced by establishing BCECF loading conditions in intact taste buds so that images at 490 and 440 nm can be acquired between 10 and 50 ms, respectively, and taking paired images at 490 and 440 nm at 15-s intervals.

Measurement of TRC [Ca^{2+}]$_i$. Relative changes in [Ca^{2+}]$_i$ were monitored in polarized TRCs by loading the tissue with Fura-2-AM (Molecular Probes). The method for loading Fura-2 and recording temporal changes in FIR (F$_{340}$/F$_{380}$) was essentially similar to that used earlier for measuring [Na$^+$]$_i$ changes with SBFI (Lyall et al., 2002b, 2005a).

Solutions. The composition of the various solutions used in the in vitro experiments is given in Table I. However, in some experiments, the control solution (C) was made hypertonic by increasing the NaCl concentration from 150 to 500 mM. In some experiments, the NH$_4$Cl concentration was varied between 0 and 25 mM. To maintain constant osmolarity, an equivalent amount of NaCl or NMDGCl was replaced with NH$_4$Cl. Some solutions contained the following drugs: ionomycin (a Ca^{2+} ionophore; 10 μM), nigericin (a K$^+$-H$^+$ exchanger; 10 μM), phalloidin (F-actin modifier; 10 μM), cytochalasin B (G-actin modifier; 20 μM). All drugs were purchased from Sigma-Aldrich and were dissolved in DMSO. The stock solutions were then mixed with appropriate solutions to achieve the final concentration of the drugs used in the experiments.

Data Analysis. Changes in TRC pH$_i$ were expressed as the mean ± SEM of *n*; where *n* represents the number of ROIs within the taste bud, M ± SEM (*n*). The changes in fluorescence intensity at 440 nm were expressed relative to the fluorescence intensity (F$_{440}$) under control conditions. The F$_{440}$ under control conditions for each ROI was taken as 100%. The data were also presented as the mean ± SEM from different tissue preparations (*N*). In this case *N* represented the number of polarized lingual preparations studied. Student's *t* test was employed to analyze the differences between sets of data.

Labeling of F- and G-actin. Fungiform taste bud fragments were harvested from isolated lingual epithelia as described before (Vinnikova et al., 2004). The isolated taste buds were placed on a CellTak (Sigma-Aldrich)-coated coverslip that formed the bottom of a perfusion chamber and were perfused with Ringer's solution (R; Table I; pH 7.4). The isolated TRCs were triple loaded with bovine pancreatic deoxyribonuclease (DNase-1) conjugated with Alexa Fluor 488, 4',6-diamidino-2-phenylin (DAPI), and rhodamine phalloidin (all from Molecular Probes) at room temperature. DNase 1 binds to monomeric G-actin, phalloidin selectively labels polymerized F-actin, and DAPI selectively binds DNA and is a nuclear stain. TRCs were treated with 0.5 μM DAPI, 10 U of rhodamine phalloidin (1.6 μM), and 0.3 μM DNase 1. DAPI and rhodamine phalloidin were dissolved in DMSO. The stock solution was then mixed with control solution (C; Table I; pH 7.4) to give the final concentration of 0.5 and 1.6 μM, respectively. A stock solution (161 μM) of DNase-1 conjugated with

Alexa 488 was made in a solution containing 20 mM Tris (pH 7.6) + 50 mM NaCl + 50% glycerol + 1 mM dithiothreitol and 0.1 mg/ml bovine serum albumin and stored at $-20°C$. The stock solution was then mixed with control solution to give the final concentration of 0.3 μM. The labeled nuclei, F-actin, and G-actin were imaged using an LSM 510 Meta confocal microscope (Carl Zeiss MicroImaging, Inc.). For DAPI the excitation wavelength was 405 nm and the emitted light was detected using a bandpass filter (420–480 nm). For rhodamine phalloidin, the excitation wavelength was 543 nm and the emitted light was detected using a bandpass filter (550–600 nm). For DNase-1 conjugated with Alexa 488 the excitation wavelength was 488 nm and the emitted light was detected using a bandpass filter 505–530 nm. The isolated taste bud fragments were visualized by taking optical sections in the Z-axis when perfused with control solution at pH 7.4 and 6.7 (C; Table I), and in the presence of 10 μM cytochalasin B (pH 7.4) or 500 mM mannitol (pH 7.4).

In Vivo Studies

CT Nerve Recordings. Female Sprague-Dawley rats (150–200 g) were anesthetized by intraperitoneal injection of pentobarbital (60 mg/kg), and supplemental pentobarbital (20 mg/kg) was administered as necessary to maintain surgical anesthesia. The animal's corneal reflex and toe-pinch reflex were used to monitor the depth of surgical anesthesia. Body temperatures were maintained at 37° with a Deltaphase Isothermal PAD (Model 39 DP; Braintree Scientific, Inc.). The left CT nerve was exposed laterally as it exited the tympanic bulla and placed onto a 32G platinum/iridium wire electrode. An indifferent electrode was placed in nearby tissue. Neural responses were differentially amplified with an optically coupled Isolated Bio-Amplifier (ISO-80; World Precision Instruments). For display, responses were filtered using a band pass filter with cutoff frequencies 40 Hz–3 kHz and fed to an oscilloscope. Responses were then full-wave rectified and integrated with a time constant of 1 s. Integrated neural responses and current and voltage changes were recorded on a chart recorder and also captured on disk using Labview software (National Instruments) and analyzed offline. Stimulus solutions were injected into a Lucite chamber (3 ml; 1 ml/s) affixed by vacuum to a 28 mm² patch of anterior dorsal lingual surface. The chamber was fitted with separate Ag-AgCl electrodes for measurement of current and potential and served as inputs to a voltage-current clamp amplifier that permitted the recording of neural responses with the chemically stimulated receptive field under zero current clamp or voltage clamp. The clamp voltages were referenced to the mucosal side of the tongue. Neural responses were recorded and analyzed as described before (Lyall et al., 2005a,b).

Solutions. The composition of the various rinse and stimulating solutions used in the CT experiments is given in Table II. CT responses to 300 mM NH$_4$Cl, 300 mM NaCl, 100 mM NaCl, 1 M mannitol (M), 10 mM quinine (Q), and 20 mM HCl were recorded with reference to 10 mM KCl rinse. In some experiments, NaCl stimulating solutions contained 5 μM benzamil (Bz; a specific blocker of the epithelial sodium channel; ENaC). The tongue was stimulated with dissolved CO$_2$ at pH 7.4 (72 mM KHCO$_3$ + 10% CO$_2$). The corresponding rinse solution contained the same concentration of KCl as KHCO$_3$ and was buffered to pH 7.4 with HEPES. The tongue was stimulated with acetic acid solutions in which 10 mM acetic acid was buffered to pH 6.1 with K-acetate. The corresponding rinse solution contained the same concentration of KCl as K-acetate and was buffered to pH 6.1 with HEPES. In some experiments both rinse and acid stimuli contained, in addition, 0.5 or 1.0 M mannitol. CT responses to the above acidic stimuli were also monitored after top-

ical application of flufenamic acid (40 μM), a specific blocker of shrinkage-activated nonselective cation channels (Koch and Korbmacher, 2000) and after application of G- and F-actin modifiers, cytochalasin B (20 μM) and phalloidin (1.2 mM), respectively. The above compounds were dissolved in DMSO and applied topically on the tongue for 30–45 min. In some experiments TRCs were loaded in vivo with a Ca^{2+} chelator, 1,2-bis(2-aminophenoxy)ethane-N,N,N',N'-tetraacetic acid tetrakis-(acetoxymethyl ester) (BAPTA-AM; Sigma-Aldrich). BAPTA-AM (30 mM) was dissolved in DMSO and applied topically to the tongue for 45 min.

Data Analysis. The numerical value of an integrated tonic CT response was obtained in the quasi-steady-state part of the response as the area under the integrated CT response curve for a time interval of 30 s measured from the end of a typical 1-min stimulation period. The phasic response was taken as the peak CT response relative to the mean steady-state (tonic) CT response. This was then normalized to the mean tonic response to 300 mM NH$_4$Cl. This normalized peak response was used to obtain an average peak response across animals. For tonic responses, changes in area under the integrated quasi-steady-state part of the CT response curves for various stimuli under different conditions were normalized to the responses observed in each animal to the tonic response of 300 mM NH$_4$Cl. Both phasic and tonic responses were expressed as the mean $\pm$ SEM of N; where N represents the number of animals in each group; M $\pm$ SEM (N). Student's t test was employed to analyze the differences between sets of data.

RESULTS

In Vitro Studies

We first investigated the relationship between pH$_i$ and cell volume in polarized TRCs using imaging techniques in vitro.

Effect of Increasing Basolateral Solution Osmolarity on TRC pH$_i$ and Volume. In TRCs loaded with BCECF (Fig. 1 A), perfusing the basolateral membrane with 500 mM NaCl produced a rapid but transient increase in F$_{440}$ (a–b; dotted line), followed by a spontaneous decrease to below its resting value (b–c). Upon reperfusing control solution there was a rapid transient decrease in F$_{440}$ (c–d), followed by a spontaneous increase to a value slightly above the resting level (d–e). Increase in F$_{440}$ indicates decrease in cell volume. A decrease in cell volume will result in an increase in dye concentration inside the cells and increase in F$_{440}$ (a–b). The spontaneous recovery of F$_{440}$ (b–c) suggests that TRCs are capable of regulatory volume increase (RVI). A decrease in F$_{440}$ as a response to lowering NaCl concentration from 500 to 150 mM is consistent with an increase in TRC volume. An increase in cell volume will result in a decrease in dye concentration inside the cells and a decrease in F$_{440}$ (c–d). The spontaneous recovery of F$_{440}$ (d–e) suggests that TRCs are capable of regulatory volume decrease (RVD).

The osmotically induced transient decrease in volume (Fig. 1 A, a–b) occurred without a significant change in TRC pH$_i$ (g–h; solid line). However, the RVI
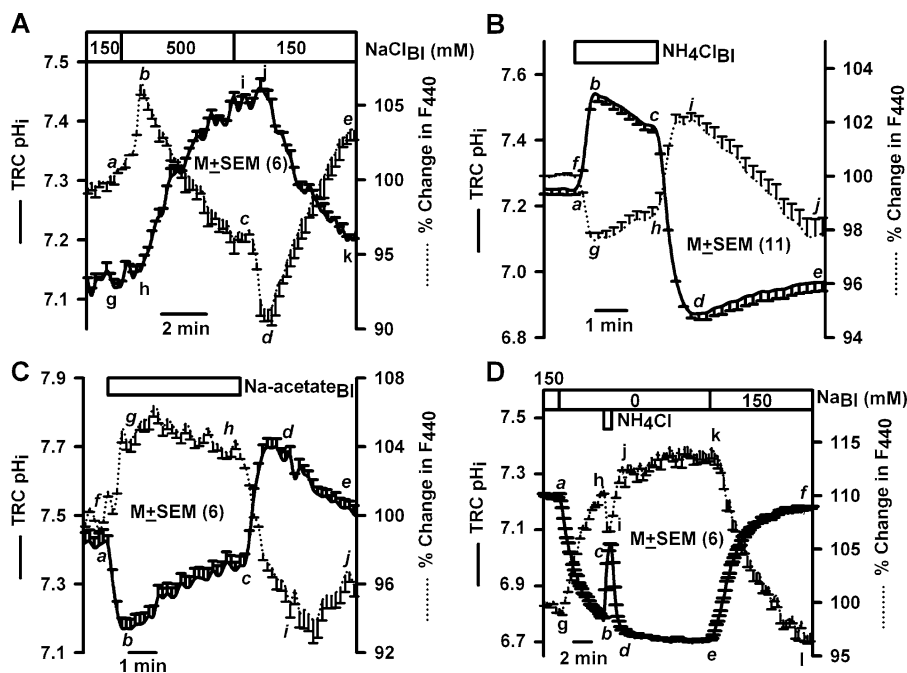
Figure 1. Effect of basolateral NaCl, NH_4Cl, and Na-acetate on TRC pH_i and volume. Lingual epithelia loaded with BCECF were initially perfused on both sides with control solution containing 150 mM NaCl (pH 7.4). During the time period shown by the top horizontal bar the basolateral membrane of polarized TRCs was perfused with (A) control solution containing 500 mM NaCl, (B) control solution containing 15 mM NH_4Cl, (C) control solution containing 15 mM Na-acetate at pH 7.4, or (D) with Na^+-free solution (0 Na_{Bl}) containing 150 mM NMDG-Cl or with Na^+-free solution containing 135 mM NMDG-Cl + 15 mM NH_4Cl (pH 7.4). Temporal changes in TRC pH_i and volume were monitored as changes in FIR (F_{490}/F_{440}, solid line) and florescence intensity of the isosbestic wavelength 440 nm (F_{440}, dotted line), respectively. The F_{440} under control conditions for each ROI was taken as 100%. Values are presented as mean ± SEM of n, where n = number of ROIs within the taste bud.

(b–c) was accompanied by an increase in pH_i (h–i). In the initial 2-min period both pH_i and F_{440} changed linearly with time ($r^2 = 0.99 \pm 0.02$; $n = 6$). Similarly, a decrease in osmolarity induced a transient increase in volume (c–d) without a significant change in TRC pH_i (i–j). However, the RVD (d–e) was accompanied by a decrease in pH_i (j–k). In the initial 1-min period, both pH_i and F_{440} changed linearly with time ($r^2 = 0.98 \pm 0.03$; $n = 6$). These results suggest that pH regulatory mechanisms in TRC membranes are involved in both RVI and RVD. In two additional polarized TRC preparations, hypertonic NaCl produced a similar relationship between pH_i and cell volume. Essentially similar results were obtained with hypertonic mannitol (unpublished data). These results are consistent with our previous studies in which TRC volume was monitored using the cell volume probe, calcein (Lyall et al., 1999) or the Na^+-sensitive dye, sodium-green (Lyall et al., 2005a). These results indicate that in BCECF-loaded TRCs, changes in F_{440} and FIR (F_{490}/F_{440}) reliably report changes in volume and pH_i, respectively.

Effect of Weak Organic Acids and Bases on TRC pH_i and Volume. At constant pH_o and osmolarity, exposing the basolateral membrane of TRCs to weak organic acids or bases induces transient changes in pH_i that recover spontaneously (Vinnikova et al., 2004). We hypothesize that at constant pH_o and osmolarity, changes in TRC pH_i will be accompanied by parallel changes in cell volume. Changes in pH_i were induced by exposing the basolateral membrane of polarized TRCs to short pulses of NH_4Cl, Na-acetate, or CO_2.

Exposing the basolateral membrane to 15 mM NH_4Cl (NH_4Cl; Table I; pH 7.4) produced a rapid intracellular alkalinization (Fig. 1 B, a–b, solid line). NH_3 diffuses across the basolateral membrane into TRCs and binds to free intracellular H^+ to form NH_4^+ and increases pH_i. This was followed by a spontaneous decrease in pH_i (b–c) due to the slower entry of NH_4^+ across the basolateral membrane and its dissociation to NH_3 + H^+. In addition, one or more pH compensatory mechanisms in TRC membranes may be involved in assisting the recovery from alkaline pH_i. Upon NH_4Cl washout, there was a rapid decrease in pH_i to below its resting value (Fig. 1 B, c–d). This is due to the rapid exit of intracellular NH_3 and the conversion of intracellular NH_4^+ to NH_3 + H^+. The loss of NH_3 from the cells results in the accumulation of excess H^+ inside the cells. The decrease in pH_i was transient and recovered spontaneously toward its resting value (Fig. 1 B, d–e). The alkalinization phase of the NH_4Cl pulse (a–b) was associated with a decrease in F_{440} (Fig. 1 B, f–g, dotted line), indicating cell swelling. The spontaneous recovery of pH_i during the NH_4Cl pulse (b–c) was accompanied by a parallel recovery of cell volume (g–h). Upon NH_4Cl washout, pH_i decreased below its resting value and was accompanied by a rapid increase in F_{440} (Fig. 1 B, h–i) that also increased (i) above its resting value (f), indicating rapid cell shrinkage. During spontaneous pH_i recovery (d–e) cell volume slowly increased toward its control value (i–j). The initial changes in pH_i, represented by a–b, b–c, c–d, and d–e, were linearly related to changes in F_{440} (mean $r^2 = 0.97 \pm 0.04$; $n = 6$). NH_4Cl pulses produced a similar relationship between

pH$_i$ and F$_{440}$ in five additional TRC preparations (see also Fig. 1 D and Fig. 2 A below).

Exposing the basolateral membrane to 15 mM Na-acetate (Table I, Na-acetate, pH 7.4) produced a rapid intracellular acidification (Fig. 1 C, a–b, solid line), due to the entry of the membrane-permeable undissociated acetic acid and its subsequent dissociation to free intracellular H$^+$ and acetate anion. Intracellular acidification was transient and demonstrated spontaneous recovery (Fig. 1 C, b–c), presumably, due to the activation of basolateral NHE-1 (Vinnikova et al., 2004). Upon Na-acetate washout, pH$_i$ alkalinized and became higher than its resting value (Fig. 1 C, c–d) due to the rapid exit of the undissociated acetic acid from cells and a decrease in intracellular H$^+$. The spontaneous recovery of alkaline pH$_i$ toward baseline (Fig. 1 C, d–e) reflects the presence of an as yet unknown pH recovery mechanism(s) in TRC membranes that allows base (OH$^-$) exit or entry of acid equivalents at alkaline pH$_i$.

Basolateral Na-acetate caused a rapid increase in F$_{440}$ (f–g, dotted line). In the initial 30-s period both pH$_i$ and F$_{440}$ changed linearly with time (r^2 = 0.82 ± 0.05; n = 6). This was followed by a partial recovery of both pH$_i$ (b–c) and F$_{440}$ toward baseline (g–h). Upon Na-acetate washout, there was a rapid transient decrease in F$_{440}$ (h–i) followed by partial recovery in cell volume (i–j). Upon Na-acetate washout, in the initial 1-min period, both pH$_i$ and F$_{440}$ changed linearly with time (r^2 = 0.97 ± 0.04; n =6). In two additional TRC preparations Na-acetate pulses produced a similar relationship between pH$_i$ and F$_{440}$. Similarly, a near linear relationship between TRC pH$_i$ and F$_{440}$ was observed during basolateral CO$_2$ pulses (unpublished data).

Effect of Basolateral Na$^+$ Removal on TRC pH$_i$ and Volume. We hypothesize that at constant pH$_o$ and osmolarity, a decrease in basolateral Na$^+$ concentration will produce a decrease in TRC pH$_i$ (Vinnikova et al., 2004) accompanied by a parallel decrease in cell volume.

Perfusing the basolateral membrane with Na$^+$-free solution (NMDGCl, Table I, pH 7.4) produced a decrease in TRC pH$_i$ (Fig. 1 D, a–b, solid line) due to the reversal of basolateral NHE-1 (Vinnikova et al., 2004). In two additional TRC preparations basolateral Na$^+$-free solution also acidified pH$_i$ and increased F$_{440}$. In the absence of Na$^+$, exposing the basolateral membrane to a short NH$_4$Cl pulse (NMDG/NH$_4$Cl, Table I, pH 7.4) produced similar changes in pH$_i$ as shown in Fig. 1 B. However, no spontaneous pH$_i$ recovery occurred in the absence of Na$^+$ (Fig. 1 D, d–e). This is because in the absence of Na$^+$, NHE-1 is inhibited. Subsequently, perfusing with control solution (C; Table I; pH 7.4) produced a rapid increase in pH$_i$ to its control value (e–f) due to the activation of NHE-1 (Vinnikova et al., 2004).
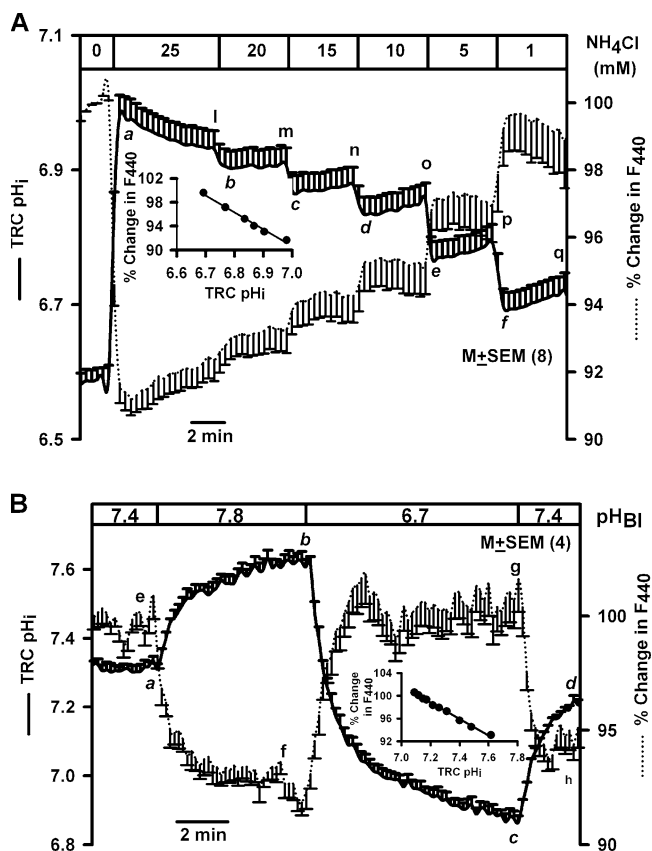

Figure 2. Effect of basolateral NH$_4$Cl concentration and pH on TRC pH$_i$ and volume. (A) A lingual epithelium loaded with BCECF was initially perfused on both sides with Na$^+$-free solution containing 150 mM NMDG-Cl (pH 7.4). All basolateral solutions contained, in addition, 10 mM BaCl$_2$, and 2 mM CPC was added to the apical solution. Temporal changes in TRC pH$_i$ and volume were monitored as changes in FIR (F$_{490}$/F$_{440}$, solid line) and fluorescence intensity of the isosbestic wavelength 440 nm (F$_{440}$, dotted line) following exposure of the basolateral membrane to 25, 20, 15, 10, 5, and 1 mM NH$_4$Cl (equivalent amount of NMDG-Cl replaced NH$_4$Cl in the basolateral solutions). The F$_{440}$ under control conditions for each ROI was taken as 100%. Inset, relationship between TRC pH$_i$ and percent change in F$_{440}$ relative to 0 NH$_4$Cl. Line of best fit was represented by the following equation: % change in F$_{440}$ = −36.3 × pH$_i$ + 343.9; r^2 = 0.99. Values are presented as mean ± SEM of n; where n = number of ROIs within the taste bud. (B) A lingual epithelium loaded with BCECF was initially perfused on both sides with control solution containing 150 mM NaCl (pH 7.4). During the time period shown by the top horizontal bar the basolateral membrane was perfused with control solution at pH 7.8, 6.7, and 7.4. Temporal changes in TRC pH$_i$ and volume were monitored as changes in FIR (F$_{490}$/F$_{440}$, solid line) and fluorescence intensity of the isosbestic wavelength 440 nm (F$_{440}$, dotted line), respectively. The F$_{440}$ under control conditions for each ROI was taken as 100%. Inset, relationship between TRC pH$_i$ and percent change in F$_{440}$ in the initial 100 s between pH$_i$ 7.6 and 7.1. Line of best fit was represented by the following equation: % change in F$_{440}$ = −14.5 × pH$_i$ + 203.2; r^2 = 0.99. Values are presented as mean ± SEM of n; where n = number of ROIs within the taste bud.

A decrease in pH_i induced by basolateral Na^+ removal increased F_{440} (Fig. 1 D, g–h, dotted line). Following Na^+ removal, in the initial 1-min period, both pH_i and F_{440} changed linearly with time ($r^2 = 0.90 \pm 0.01$; $n = 6$), indicating that a decrease in pH_i causes cell shrinkage. In the absence of Na^+, basolateral NH_4Cl pulse initially produced a rapid decrease in F_{440} (h–i) and, upon NH_4Cl washout, increased F_{440} (j) above its value just before the pulse (h). In the absence of Na^+, no recovery was observed in either pH_i (d–e) or F_{440} (j–k). Na^+ addition produced pH_i recovery (e–f) and a decrease in F_{440} (k–l). In the initial 2-min period, both pH_i and F_{440} changed linearly with time ($r^2 = 0.92 \pm 0.04$; $n = 6$), indicating that an increase in pH_i causes cell swelling.

Effect of Step Changes in Basolateral NH_4Cl Concentration on TRC pH_i and Volume. We hypothesize that at constant pH_o and osmolarity, step changes in basolateral NH_4Cl concentration will produce graded changes in TRC pH_i (Vinnikova et al., 2004) accompanied by parallel graded changes in cell volume. During step changes in NH_4Cl both the pH_i recovery and the NH_4^+ loss from the cells were minimized. pH_i recovery was inhibited by perfusing the tissue with Na^+-free solution (compare Fig. 1 D). NH_4^+ loss through apical VR-1 variant cation channels and basolateral K^+ channels was minimized by adding 2 mM cetylpyridinium chloride (CPC) and 10 mM $BaCl_2$ to the apical and basolateral solution, respectively (Vinnikova et al., 2004).

Exposing the basolateral membrane to 25 mM NH_4Cl ($NMDG/NH_4Cl$, Table I, pH 7.4) induced a rapid increase in mean pH_i from 6.58 to 6.98 (Fig. 2 A, solid line, point a) and decreased F_{440} by ~8%, indicating cell swelling. Decreasing the NH_4Cl concentration in a stepwise manner produced a graded decrease in pH_i (at time points b, c, d, e, and f) with minimal spontaneous pH_i recovery and a rapid and graded increase in F_{440}. At time points a, b, c, d, e, and f there was a linear relationship between pH_i and F_{440} (Fig. 2, inset; $r^2 = 0.98$; $n = 8$). There was also a linear relationship between pH_i and F_{440} at the time points represented by l, m, n, o, p, and q, during which small, but significant, spontaneous pH_i recovery was observed. This pH_i recovery is due to one or more Na^+-independent pH recovery mechanisms in TRC membranes. Similar results were obtained in two additional TRC preparations.

Effect of pH_o on TRC pH_i and Volume. We hypothesize that changes in either apical or basolateral pH will induce changes in TRC pH_i (Lyall et al., 2001, 2002b) accompanied by parallel changes in cell volume. Elevating basolateral pH from 7.4 to 7.8 (Fig. 2 B) increased TRC pH_i (a–b, solid line) and cell volume (e–f, dotted line). Lowering basolateral pH from 7.8 to 6.7 decreased pH_i (b–c) and decreased cell volume (f–g). In the initial
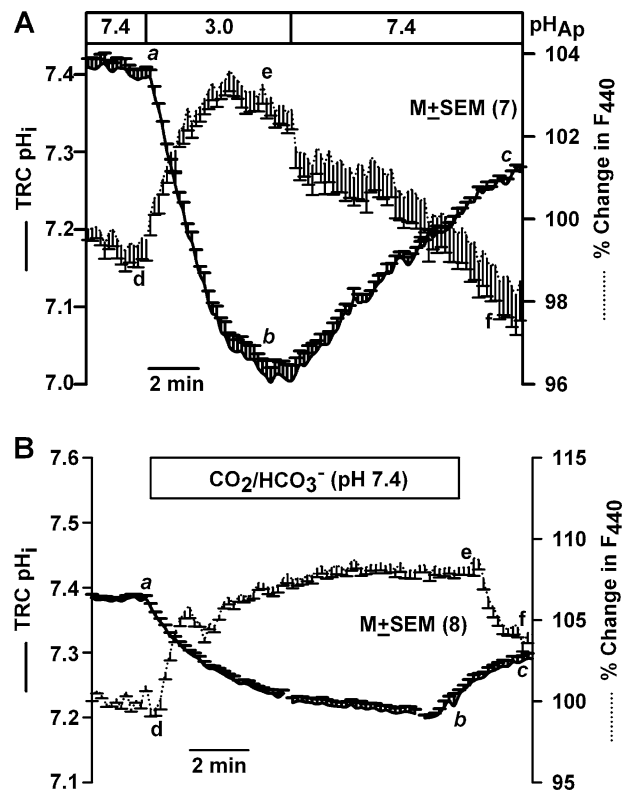

Figure 3. Effect of apical pH on TRC pH_i and volume. A lingual epithelium loaded with BCECF was initially perfused on both sides with control solution containing 150 mM NaCl (pH 7.4). (A) During the time period shown by the top horizontal bar, the apical membrane was perfused with an unbuffered solution containing 1 mM HCl (pH 3). (B) During the time period shown by the top horizontal bar, the apical membrane was perfused with a HEPES-free solution in which 72 mM NaCl was replaced with 72 mM $NaHCO_3$. The pH of this solution was adjusted to 7.4 by continuously bubbling with 10% CO_2. Temporal changes in TRC pH_i and volume were monitored as changes in FIR (F_{490}/F_{440}, solid line) and fluorescence intensity of the isosbestic wavelength 440 nm (F_{440}, dotted line), respectively. The F_{440} under control conditions for each ROI was taken as 100%. In each case the values are presented as mean ± SEM of n, where n = number of ROIs within the taste bud.

100 s, changes in TRC pH_i between 7.6 and 7.1 produced a linear change in F_{440} (Fig. 2 B, inset; $r^2 = 0.99 \pm 0.01$; $n = 4$). It should be noted that changes in basolateral pH induced sustained changes in pH_i and cell volume (see also Fig. 6).

The relationship between basolateral pH, TRC pH_i, and cell volume shown in Fig. 2 B was not affected by replacing 50 mM NaCl with 50 mM KCl in the basolateral solution (unpublished data). An increase in basolateral K^+ concentration is expected to depolarize the membrane potential, suggesting that the relationship between pH_i and cell volume is indifferent to changes in membrane potential. The relationship between basolateral pH, TRC pH_i, and cell volume was also not altered in the absence of Cl^- (unpublished data).

Similarly, during calibration of the pH using high K^+ solutions plus nigericin (HK; Table I), changes in pH_i between 6.7 and 7.8 also demonstrated a linear relationship with changes in F_{440} ($r^2 = 0.96 \pm 0.04$; $n = 6$). In the presence of high K^+, membrane potential depolarizes to 0 mV and nigericin causes equilibration of pH_i with pH_o. Under these conditions there is no pH gradient, and no pH or volume regulatory mechanisms are operative.

Perfusing the apical membrane with HCl (HCl, Table I, pH 3) induced a sustained decrease in resting TRC pH_i (Fig. 3 A, a–b) and a sustained decrease in cell volume (d–e). In the initial 100 s, changes in TRC pH_i produced a linear change in F_{440} ($r^2 = 0.97 \pm 0.01$; $n = 7$). Changes in pH_i (b–c) and volume (e–f) recovered upon reperfusing the apical membrane with control solution (pH 7.4). Similar results were obtained with acetic acid, pH 3.0 (unpublished data).

In a lingual epithelium initially perfused on both sides with HEPES-buffered control solution (C, Table I, pH 7.4), switching to a similar solution buffered with CO_2/HCO_3^- (CO_2/HCO_3^-, Table I, pH 7.4) on the apical side reversibly decreased TRC pH_i (Fig. 3 B, a–b–c). A decrease in TRC pH_i (Fig. 3 B, a–b) was accompanied by an increase in F_{440} (d–e), indicating cell shrinkage. Thus both strong and weak acids decrease pH_i and decrease TRC volume independent of the stimulus pH.

Effect of Changes in $[Ca^{2+}]_i$ on TRC pH_i and Volume. Changes in $[Ca^{2+}]_i$ modulate TRC pH_i (Lyall et al., 2002a; 2004a). We hypothesize that changes in TRC $[Ca^{2+}]_i$ will also induce parallel changes in cell volume. In a polarized TRC preparation loaded with Fura-2, basolateral ionomycin (10 μM) produced a reversible increase in FIR (Fig. 4 A, F_{340}/F_{380}, a–b) and hence reversibly increased $[Ca^{2+}]_i$. Ionomycin alkalinized resting TRC pH_i (Fig. 4 B, a–b, solid line) and decreased F_{440} (d–e, dotted line), indicating cell swelling. In the initial 100 s following ionomycin treatment there was a linear relationship between the increase in pH_i and the decrease in F_{440} ($r^2 = 0.95 \pm 0.05$; $n = 6$). Similarly, upon ionomycin washout, pH_i decreased with an increase in F_{440}, indicating cell shrinkage. Ionomycin produced similar effects in two additional TRC preparations. Ionomycin induced intracellular alkalinization by increasing the rate of pH_i recovery from an NH_4Cl pulse (Fig. 4 C). Under control conditions, the mean pH_i recovery rate was 0.038 ± 0.003 pH_i/min (c–d) and was significantly increased to 0.11 ± 0.003 pH_i/min (g–h) after the ionomycin treatment ($P < 0.01$, $n = 10$, paired). An increase in $[Ca^{2+}]_i$ activates NHE-1 (Lyall et al., 2002a, 2004a).

Effect of pH on F- and G-actin in Isolated Taste Bud Fragments. Major cell cytoskeletal proteins have been localized in TRCs (Hofer and Drenckhahn, 1999; Ohishi et
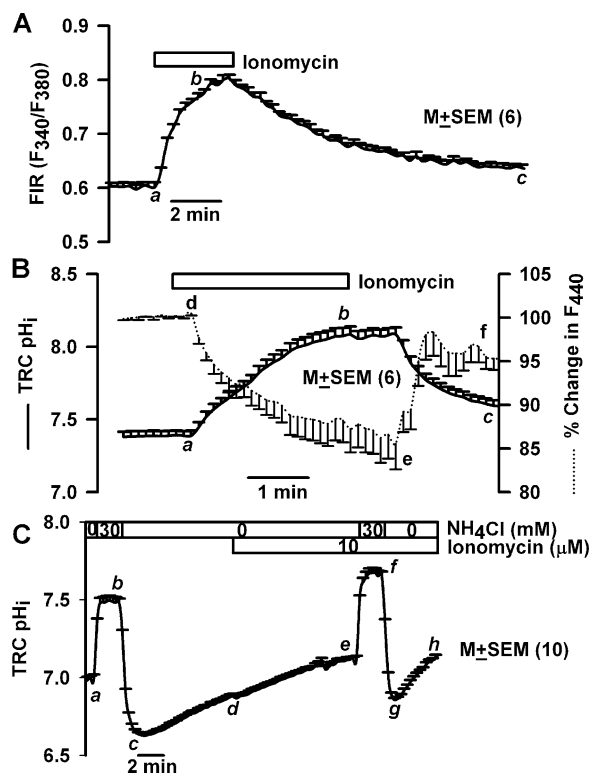

Figure 4. Effect of changes in $[Ca^{2+}]_i$ on TRC pH_i and volume. (A) A lingual epithelium loaded with Fura-2 was initially perfused on both sides with control solution containing 150 mM NaCl (pH 7.4). During the time period shown by the top horizontal bar, the basolateral membrane was perfused with the control solution containing, in addition, 10 μM ionomycin. Changes in TRC $[Ca^{2+}]_i$ were monitored as temporal changes in FIR (F_{340}/F_{380}). (B and C) Lingual epithelium loaded with BCECF was initially perfused on both sides with control solution containing 150 mM NaCl (pH 7.4). During the time period shown by the top horizontal bar the basolateral membrane was perfused with the control solution containing, in addition, 10 μM ionomycin. Temporal changes in TRC pH_i and volume were monitored as changes in FIR (F_{490}/F_{440}, solid line) and fluorescence intensity of the isosbestic wavelength 440 nm (F_{440}, dotted line). The F_{440} under control conditions for each ROI was taken as 100%. In C the spontaneous pH_i recovery rates were monitored by the NH_4Cl pulse technique before (c–d) and after ionomycin treatment (g–h). In each case the values are presented as mean $\pm$ SEM of n, where n = number of ROIs within the taste bud.

al., 1999; Sekerkova et al., 2004). We hypothesize that one of the ways that changes in pH_i can modulate cell volume rapidly is by interacting with the cytoskeleton and altering cell structure. The actin cytoskeleton of TRCs was visualized using specific fluorescent probes for both monomeric (G)-actin and filamentous (F)-actin. Fig. 5 (A–E) shows a confocal image of an optical plane through an isolated fungiform taste bud fragment perfused with control solution (C, Table I, pH 7.4). The figure shows F-actin binding to rhodamine phalloidin (A, red), transmitted image (B); G-acting binding to pancreatic DNase 1 conjugated with Alexa 488 (C, green);
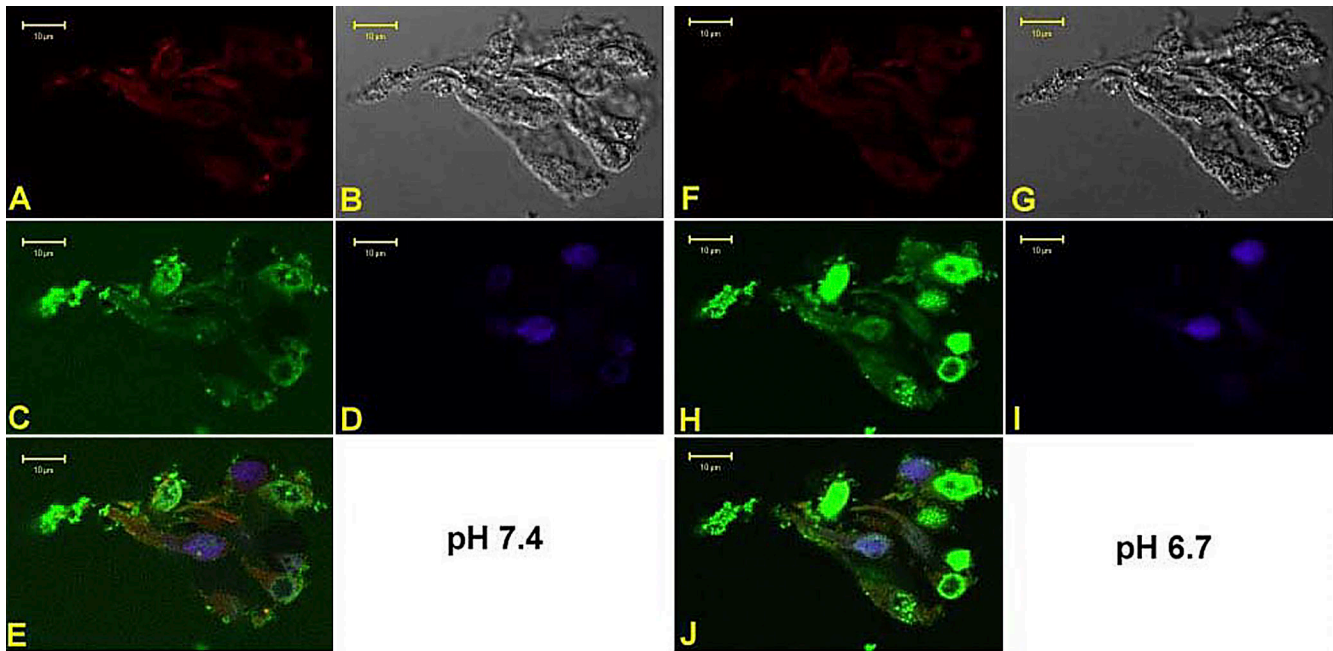
Figure 5. Labeling of F- and G-actin in an isolated fungiform taste bud fragment at pH 7.4 and 6.7. A confocal image of an optical plane of a fungiform taste bud fragment showing F-actin binding to rhodamine phalloidin (A and F, red), transmitted image (B and G), G-actin binding to pancreatic DNase 1 conjugated with Alexa 488 (C and H, green), staining of TRC nuclei with DAPI (D and I, blue), and an overlay of all images (E and J) are shown while the taste bud was perfused with control solution at pH 7.4 (A–E) or pH 6.7 (F–J).

staining of TRC nuclei with DAPI (D, blue), and an overlay of all images (E). In individual TRCs both F-actin and G-actin are present in the apical region, basolateral region, and the soma surrounding the nuclei. Lowering pH from 7.4 to 6.7 for 1 min (Fig. 5, F–J) produced a decrease in F-actin label (A versus F) and increased G-actin labeling (C versus H). The increase in G-actin was more pronounced in the soma surrounding the cell nuclei. However, it should be pointed out that the increase in G-actin label at pH 6.7 was observed only in a subset of TRCs. This suggests that a decrease in pH_i induces changes in cell volume by interacting with the actin cytoskeleton in a subset of TRCs. Similar results were obtained in two additional fungiform taste bud fragments. Treating the taste bud fragments with 20 μM cytochalasin B decreased F-actin (unpublished data). In addition, in taste bud fragments pretreated with 20 μM cytochalasin B or 10 μM phalloidin, a decrease in basolateral pH from 7.4 to 6.7 did not produce a decrease in F-actin or an increase in G-actin label (unpublished data). We hypothesize that changes in the actin cytoskeleton of TRCs will inhibit pH_i-induced changes in cell volume.

Effect of F- and G-actin Probes and Mannitol on TRC pH_i and Volume. Exposing TRCs to 10 μM phalloidin for 10 min did not affect the magnitude of pH_i change induced by a decrease in basolateral pH from 7.4 to 7.0 (Fig. 6 A, d–e) relative to control (a–b). However, the pH_i-induced changes of F_{440} were 50% smaller relative to

control in the presence of phalloidin (m–n versus j–k). Similarly, treating TRCs with 20 μM cytochalasin B for 20 min (Fig. 6 B) also inhibited the pH_i-induced increase in F_{440} (j–k) by 40% relative to control (g–h). This indicates that alteration in cell actin cytoskeleton modulates pH_i-induced changes in TRC volume.

In Vivo Studies
A decrease in TRC pH_i is the proximate stimulus for sour taste transduction (Lyall et al., 2001). Since changes in TRC pH_i demonstrate a linear relationship with cell volume (compare Figs. 1–4 and 6), we hypothesize that a decrease in cell volume is an essential intracellular intermediate signaling event during acid taste transduction. To test this hypothesis, CT responses to acidic stimuli were monitored in the presence of hypertonic mannitol and F- and G-actin modifiers.

Effect of Hypertonic Mannitol on the CT Response to Acidic Stimuli. We preshrank TRCs by superfusing the tongue with the rinse solution (R) containing 1 M mannitol. Replacing the rinse with an isosmotic and iso-pH CO_2/HCO_3^- buffered solution (Table II; pH 7.4) elicited a CT response that is composed of two components with distinct temporal characteristics. A rapid transient increase in the phasic neural response (Fig. 7 A, a–b), which declined to a quasi-steady state after ~2–5 s (b–c), defined as the tonic phase of the CT response (c–d). Repeatedly stimulating the tongue with dissolved
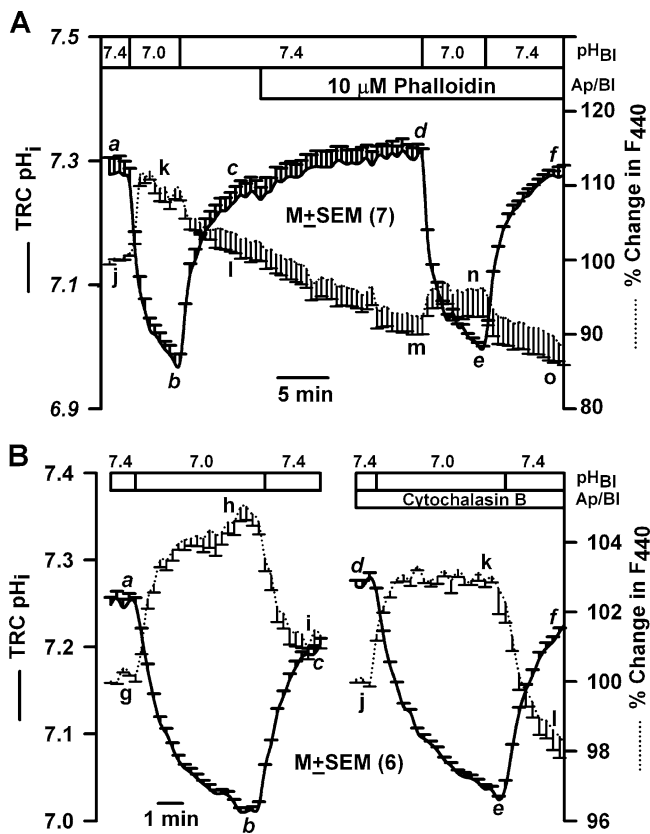
Figure 6. Effect of phalloidin and cytochalasin B on TRC pH_i and volume. A lingual epithelium loaded with BCECF was initially perfused on both sides with control solution containing 150 mM NaCl (pH 7.4). (A) At the time period shown by the top horizontal bar, both the apical and basolateral membranes were perfused with control solution containing 10 μM phalloidin (pH 7.4). In B, both sides of the epithelium were exposed to 20 μM cytochalasin B for 20 min (pH 7.4). Temporal changes in TRC pH_i and volume were monitored as changes in FIR (F_{490}/F_{440}, solid line) and the fluorescence intensity of the isosbestic wavelength 440 nm (F_{440}, dotted line), respectively, as a response to a decrease in the basolateral pH from 7.4 to 7.0. The F_{440} under control conditions for each ROI was taken as 100%. In each case the values are presented as mean ± SEM of n, where n = number of ROIs within the taste bud.

Figure 7. Effect of hypertonic mannitol on the CT response to CO_2 and HCl. (A) The CT responses to dissolved CO_2 (72 mM $KHCO_3$ + 10%/90% CO_2/O_2; pH 7.4) were recorded relative to the rinse solution, R (72 mM KCl + 10 mM HEPES; pH 7.4). In the second part of the experiment the CT responses were recorded with both rinse (R+M) and the CO_2 solution (M+CO_2) containing, in addition, 1 M mannitol (M). (B) Inset shows a set of transient phasic responses to CO_2 stimulation in the presence and absence of mannitol in an extended time scale. The magnitude of the peak phasic response was normalized to the phasic response elicited by stimulation with 300 mM NH_4Cl. (C) The CT responses to 20 mM HCl + 10 mM KCl (R+HCl) were recorded relative to the rinse solution, R (10 mM KCl). In the second part of the experiment the CT responses were recorded with both rinse (R+M) and the HCl solution (R+M+HCl) containing, in addition, 1 M mannitol (M). The arrows indicate the time when the tongue was superfused with different solutions.

CO_2 produced almost identical CT response profiles. Replacing the rinse (R) with another rinse containing 1 M mannitol (R+M; pH 7.4) produced a transient phasic response (e–f) that spontaneously decreased to rinse level. Replacing R+M with dissolved CO_2 solution containing mannitol (M+CO_2; pH 7.4) produced a CT response in which the phasic part of the neural response relative to the tonic part (h–i) was 65% smaller relative to control (b–c). For comparison, a set of transient phasic responses to CO_2 stimulation in the presence and absence of mannitol are shown in Fig. 7 B in an extended time scale. Hypertonic mannitol did not affect the tonic part of the CT response (i–j) relative to control (c–d). Repeatedly stimulating the tongue with
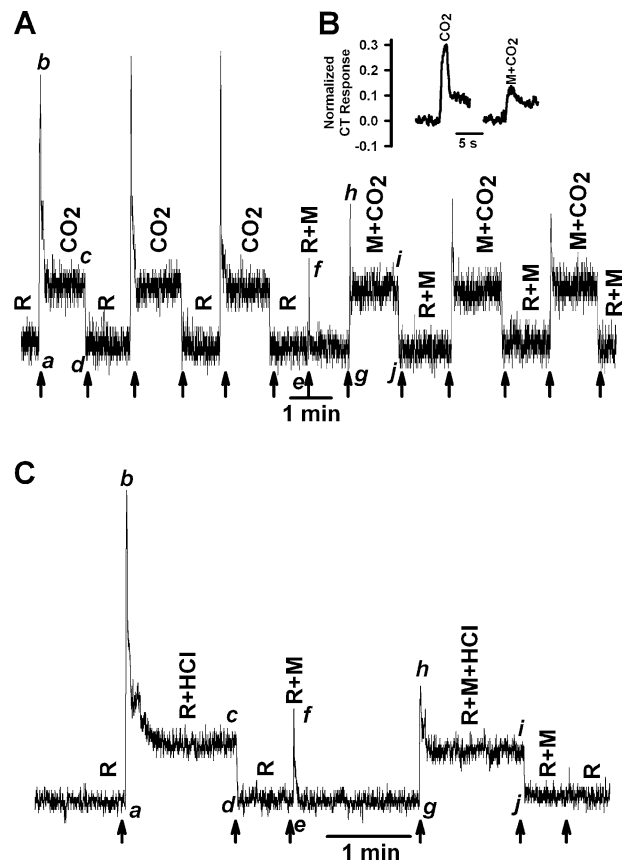
M+CO_2 produced almost identical CT response profiles. Similar results were obtained with 10 mM acetic acid (Table II; pH 6.1) (unpublished data).

Stimulating the tongue with 20 mM HCl + 1 M mannitol (R+M+HCl) also elicited a CT response in which the phasic part of the CT response relative to the tonic part (Fig. 7 C, h–i, R+M+HCl) was decreased by 78% relative to its value in the absence of mannitol (Fig. 7 C, b–c, R+HCl). Mannitol produced only minimal effects on the tonic part of the HCl CT response (i–j) relative to control (c–d). These results indicate that the phasic part of the CT response to both strong and weak acid

TABLE II
Composition of Solutions Used in In Vivo Experiments

Rinse (R)	Stimulus solution (S)
mM	*mM*
10 KCl	300 NH$_4$Cl, 300 NaCl
10 KCl	10 KCl + 100 NaCl[a]
10 KCl	10 KCl + 20 HCl
10 KCl	10 KCl + 10 quinine
72 KCl + 10 HEPES, pH 7.4	72 KHCO$_3$ + 10% CO$_2$, pH 7.4
175 KCl + 10 HEPES, pH 6.1	175 K-acetate + 10 acetic acid, pH 6.1

[a]In some experiments 5 μM Bz was added to the NaCl stimulating solutions. In some experiments 0.5 or 1.0 M mannitol was added to both rinse and stimulating solutions.

Figure 8. Effect of hypertonic mannitol on the CT response to NaCl, NH$_4$Cl, and quinine. (A) The CT responses to 100 mM NaCl + 10 mM KCl (R+N) were recorded relative to the rinse solution, R (10 mM KCl). In the second part of the experiment the CT responses were recorded with both rinse (R+M) and the NaCl solution (R+N+M) containing, in addition, 1 M mannitol (M). (B) The CT responses to 100 mM NaCl + 10 mM KCl + 5 μM Bz (N+Bz), 10 mM KCl + 10 mM quinine (Q), or 0.3 M NH$_4$Cl were recorded relative to the rinse solution, R (10 mM KCl) in the absence and presence of 1 M mannitol (M). In the second part of the experiment CT responses to the above stimuli were again recorded in the same animal after the topical lingual application of 20 μM cytochalasin B for 20 min. The arrows indicate the time when the tongue was superfused with different solutions.

stimulation is attenuated by increasing the osmolarity of the stimulating solution with mannitol.

Effect of Hypertonic Mannitol on the CT Response to NaCl and Quinine. Stimulating the tongue with 10 mM KCl rinse solution containing 1 M mannitol (R+M; Table II) and then with the NaCl stimulating solution containing 10 mM KCl + 100 mM NaCl + 1 M mannitol (R+N+M) elicited a CT response (Fig. 8 A) in which both the phasic part of the response (g–h) and the tonic part of the response (i–j) were greater relative to their respective values (a–b) and (c–d) in the absence of mannitol. Repeatedly stimulating the tongue with R+N+M produced almost identical CT response profiles. Similar results were obtained with hypertonic cellobiose (Lyall et al., 1999). In contrast, hypertonic urea did not affect CT responses to NaCl (Lyall et al., 1999) or to acidic stimuli (unpublished data). These results indicate that in contrast to acidic stimuli, hypertonic mannitol increases the phasic and tonic components of the CT response to NaCl.

Hypertonic mannitol had no effect on either the phasic or the tonic component of the CT response to 100 mM NaCl + 5 μM Bz (N+Bz+M) relative to its value in the absence of mannitol (N+Bz) (Fig. 8 B). Thus mannitol specifically increases both the phasic and the tonic component of the Bz-sensitive NaCl CT response derived from Na$^+$ flux through apical ENaC (Lyall et al., 1999). In contrast, mannitol does not affect the Bz-insensitive NaCl CT response derived from Na$^+$ flux through the TRPV1 variant salt taste receptor (Lyall et al., 2004b). Hypertonic mannitol had no effect on either the phasic or the tonic component of the CT response to 10 mM quinine (Q+M) relative to its values in the absence of mannitol (Q), indicating that the transduction mechanism for quinine does not involve cell shrinkage. Thus an increase in osmolarity specifically decreases the magnitude of the phasic response to acidic stimuli through cell shrinkage.
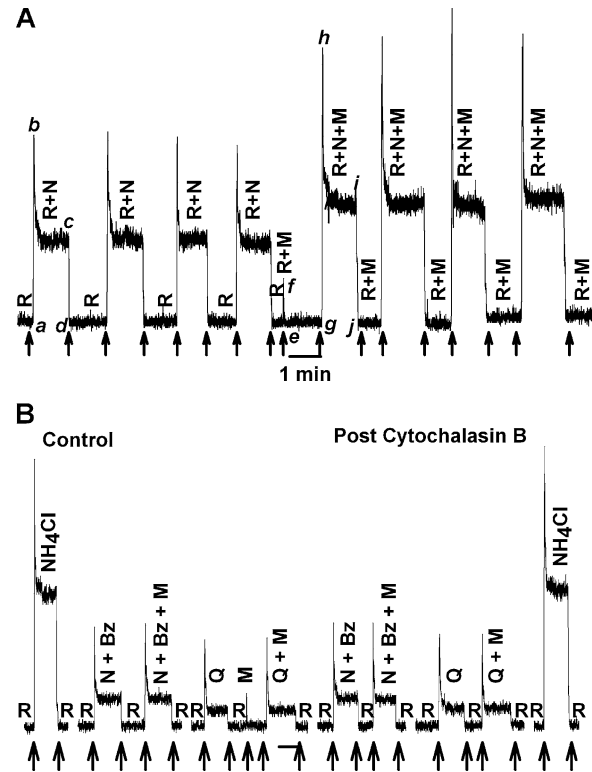
Effect of F- and G-actin Probes on the CT Response to Acidic Stimuli. Cytochalasin B shifts the equilibrium from F-actin to G-actin and inhibits the pH$_i$-induced decrease in cell volume (Fig. 6 B). Superfusing the tongue with dissolved CO$_2$ solution containing 1 M mannitol decreased the magnitude of the phasic response relative to the tonic response (Fig. 9 A, f–g) compared with control (b–c). Cytochalasin B (Fig. 9 A, post-cytochalasin B) inhibited the phasic part of the CT response by >80% (j–k) relative to control (b–c). Cytochalasin B produced no effect on the tonic part of the CT response (k–l versus c–d). After cytochalasin B treatment, increasing the osmolarity of the CO$_2$ solution with 1 M mannitol (M+CO$_2$) completely eliminated the phasic part of the CT response (n–o) relative to control (f–g). Cytochalasin B also diminished the response to rinse + mannitol (R+M) relative to rinse alone (R). This indicates that
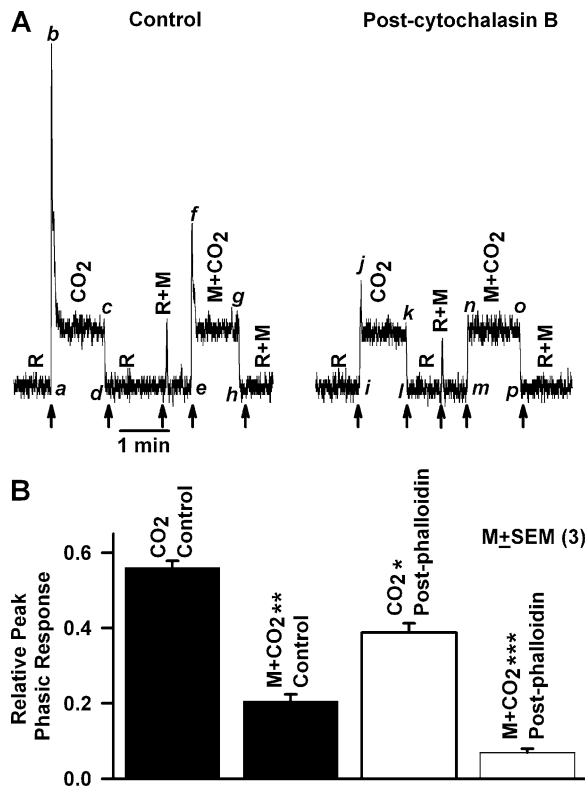
Figure 9. Effect of cytochalasin B and phalloidin on the CT response to CO_2. The CT responses to dissolved CO_2 (72 mM $KHCO_3$ + 10%/90% CO_2/O_2; pH 7.4) were recorded relative to the rinse solution, R (72 mM KCl + 10 mM HEPES; pH 7.4) before and after the topical lingual application of (A) 20 μM cytochalasin B for 20 min or (B) 1.2 mM phalloidin for 30 min. The CT responses were recorded also with both rinse (R+M) and the CO_2 solution (M+CO_2) containing, in addition, 1 M mannitol (M). The arrows indicate the time when the tongue was superfused with different solutions. In B, the peak CT response data were normalized to the tonic 300 mM NH_4Cl response in each animal (as described in the MATERIALS AND METHODS section) and are presented as the mean ± SEM of the relative peak phasic response from three animals. *, P < 0.05; **, P < 0.01; ***, P < 0.001.

Figure 10. Effect of cytochalasin B and phalloidin on the CT response to HCl. (A) The CT responses to 20 mM HCl + 10 mM KCl (R+HCl) were recorded relative to the rinse solution, R (10 mM KCl). CT responses were also recorded with both rinse (R+M) and the HCl solution (R+M+HCl) containing, in addition, 500 mM mannitol (M). CT responses were recorded under control conditions (Control), after topical lingual application of 20 μM cytochalasin B for 20 min (Post-cyto B), and after topical lingual application of 1.2 mM phalloidin for 30 min (Post-cyto B and phalloidin). (B) Summary of the effect of cytochalasin B and phalloidin on the CT response to HCl. The relative peak phasic responses (a–b, c–d, e–f, g–h, i–j, and k–l) from three animals were normalized to tonic 300 mM NH_4Cl in each individual animal and presented as mean ± SEM for control (black bar), post-cytochalasin (white bar), and post-cytochalasin B and phalloidin treatment (hatched bar). *, P < 0.05; **, P < 0.01; ***, P < 0.001.

interfering with the cell cytoskeleton also attenuates the osmotically induced decrease in TRC volume.

Phalloidin binds to F-actin and stabilizes the cell cytoskeleton and inhibits the pH_i-induced decrease in cell volume (Fig. 6 A). In three animals, treating the lingual surface with 1.2 mM phalloidin for 45 min also inhibited the phasic part of the CT response to CO_2 (Fig. 9 B, CO_2 post-phalloidin, open bar) relative to control (CO_2 control, filled bar). After phalloidin treatment, hypertonic mannitol (M+CO_2 post-phalloidin, open bar) also produced a significantly greater inhibition (P < 0.001, N = 3) of the phasic response relative to control (M+CO_2 control, filled bar).

CT responses to 20 mM HCl were recorded under control conditions, after topical lingual application of 20 μM cytochalasin B for 20 min and then after treat-
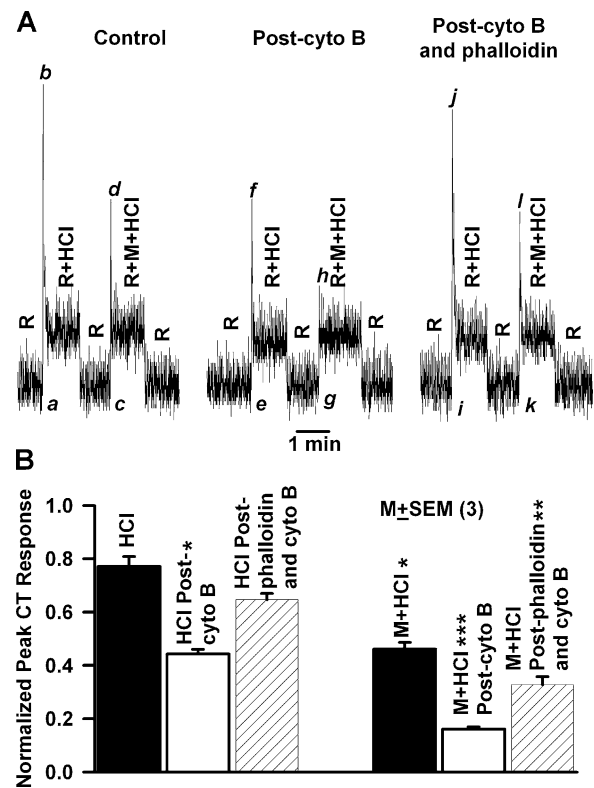
ing the tongue with 1.2 mM phalloidin for additional 40 min. Cytochalasin B inhibited the phasic part of the HCl CT response relative to the tonic part (Fig. 10 A, peak [f] to tonic level) relative to control (peak [b] to tonic level). In the presence of 1 M mannitol (R+M+HCl), the post-cytochalasin B phasic response to HCl (peak [h] to tonic level) was almost eliminated relative to control (peak [d] to tonic level). Subsequently treating the tongue with phalloidin, both the magnitude of the phasic part of the CT response to HCl in the absence (Fig. 10 A; peak [j] to tonic level) and presence of mannitol (peak [l] to tonic level) increased to near control levels. The data from three such experiments are summarized in Fig. 10 B and indicate that phalloidin partially reverses the attenuation in the phasic part of the

CT response to HCl alone and to stimulation with M+HCl (hatched bars) caused by cytochalasin B pretreatment (open bars). Thus mannitol and the decrease in pH$_i$ produce additive effects on TRC volume.

Cytochalasin B had no effect on the CT responses to 100 mM NaCl + 5 μM Bz (N+Bz), 10 mM quinine (Q), or 300 mM NH$_4$Cl relative to control (Fig. 8 B). This indicates that changes in cytoskeleton specifically modulate the phasic part of the CT response to acidic stimuli and do not affect other taste modalities.

Relationship between pH$_i$ Decrease, Changes in Cell Cytoskeleton, Cell Shrinkage, and Membrane Conductance. We hypothesize that pH$_i$-induced changes in the cell cytoskeleton activate a membrane conductance in TRCs that is involved in the phasic response to acidic stimuli. To detect the presence of a membrane conductance activated during the phasic response, CT responses to HCl were monitored under lingual voltage clamp. Just before superfusing the tongue with 20 mM HCl, during the rinse (10 mM KCl) a transepithelial voltage of −60 or +60 mV was applied across the tongue (Fig. 11 A, arrows). We reasoned that any conductance that is activated during pH$_i$-induced cell shrinkage should be voltage sensitive, and hence, should affect the phasic part of the CT response to acid stimulation. Second, in TRCs that are preshrunken with hypertonic mannitol, this conductance will either not be activated by acid stimulation or its activation will be significantly reduced. Imposing a −60 mV transepithelial potential across the tongue (Fig. 11 A) did not affect the magnitude of the phasic response (−60 mV) relative to zero current clamp (0 mV). In contrast, imposing a +60 mV transepithelial potential enhanced the magnitude of the phasic part of the CT response (+60 mV) by almost twofold relative to 0 mV (0 mV). In the presence of 1 M mannitol, the phasic responses at 0, −60, and +60 mV were attenuated relative to control. In addition, hypertonic mannitol (M+HCl) almost completely inhibited the increase in the magnitude of the phasic part of the CT response at +60 mV applied transepithelial potential (Fig. 11 A). It should be noted that both the applied transepithelial potential and the hypertonic mannitol produced only minimal effects on the tonic part of the CT response to HCl. The magnitude of the peak phasic response to HCl was monitored for a range of voltages between −80 and +80 mV in three animals. The results demonstrate that the membrane conductance becomes activated at positive voltages (Fig. 11 B, ●). Preshrinking TRCs with hypertonic mannitol inhibited the membrane conductance at all voltages (Fig. 11 B, ○). This suggests the possibility that the membrane conductance activated during acid transduction is most likely activated due to pH$_i$-induced cell shrinkage.
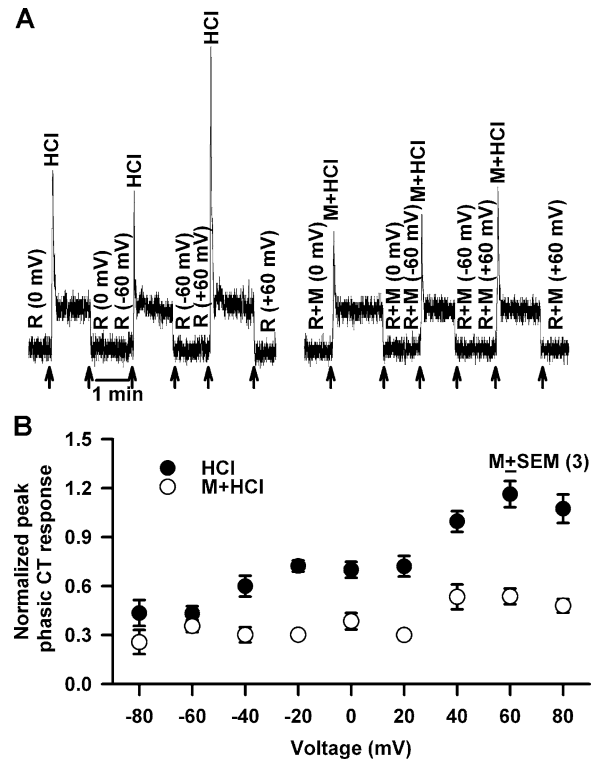

Figure 11. Effect of voltage on the phasic response to HCl stimulation in the absence and presence of hypertonic mannitol. (A) The CT responses to 20 mM HCl were recorded relative to the rinse (R = 10 mM KCl) in the presence (M+HCl) and absence (HCl) of 1 M mannitol (M). Just before superfusing the tongue with HCl, during perfusion of the tongue with the rinse solution a transepithelial voltage of either −60 or +60 mV was applied across the receptive field (arrows). (B) Summary of the osmotic effect of mannitol on the CT response to HCl at each applied transepithelial voltage between −80 and +80 mV. The relative peak phasic responses to HCl from three animals were normalized to the tonic 300 mM NH$_4$Cl response in each individual animal and presented as mean ± SEM at each voltage in the absence (●) and presence (○) of mannitol.

Several epithelial as well as nonepithelial cells contain shrinkage-activated nonselective cation channels (Koch and Korbmacher, 1999, 2000). These channels discriminate poorly between NH$_4^+$, Na$^+$, K$^+$, and Li$^+$ ions but are not permeable to divalent cations and can be blocked specifically by flufenamic acid. Most importantly, modifying the cytoskeleton with cytochalasin D and taxol inhibited the nonselective cation channels (Koch and Korbmacher, 2000). Therefore, we tested the possibility that flufenamic acid–sensitive nonselective cation channels are activated by pH$_i$-induced TRC shrinkage.

Topical lingual application of flufenamic acid (40 μM) for 20 min (Fig. 12) inhibited the phasic part of the CT response to HCl relative to the tonic part (l–m) compared with control (b–c). In the presence of 1 M mannitol, the post-flufenamic acid phasic response to
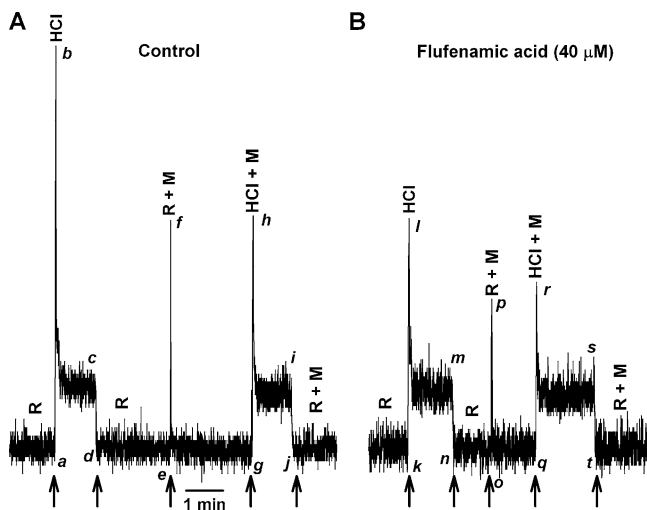
Figure 12. Effect of flufenamic acid on the CT response to HCl. CT responses to 20 mM HCl were monitored in the absence and presence of 1 M mannitol (M) before (A) and after (B) treating the tongue with 40 μM flufenamic acid for 20 min. The arrows represent the time periods at which the tongue was superfused with different solutions.
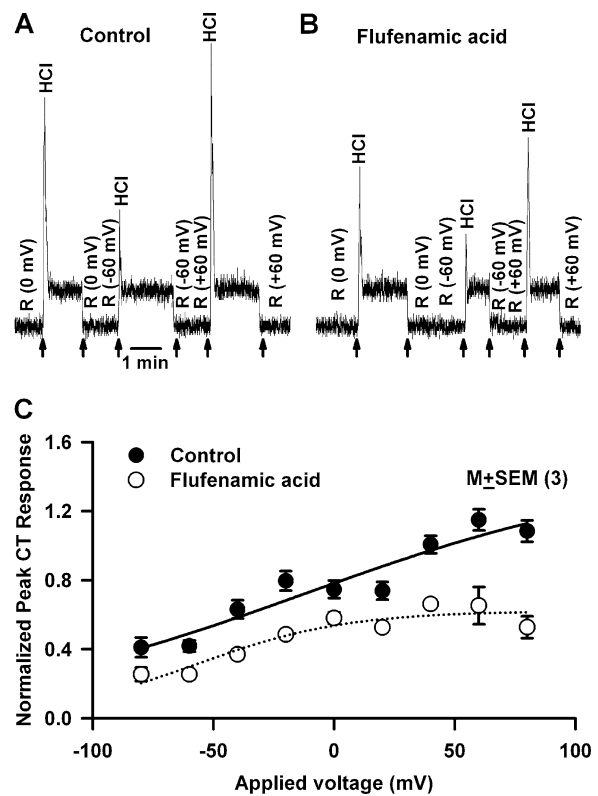

Figure 13. Effect of applied voltage on the phasic response to HCl stimulation in the presence and absence of flufenamic acid. The CT responses to 20 mM HCl were recorded relative to the rinse (R = 10 mM KCl) before (A) and after (B) treating the tongue with 40 μM flufenamic acid for 20 min. Just before superfusing the tongue with HCl, during perfusion of the tongue with the rinse solution a transepithelial voltage of either −60 or +60 mV was applied across the receptive field. The arrows represent the time periods at which the tongue was superfused with HCl. (C) The CT responses to 20 mM HCl were recorded relative to the rinse (R = 10 mM KCl) before and after treating the tongue with 40 μM flufenamic acid for 20 min. Just before superfusing the tongue with HCl, during perfusion of the tongue with the rinse solution, a transepithelial voltage between −80 or +80 mV was applied across the receptive field. For each voltage step the magnitude of the peak phasic response was calculated. The peak CT response data were normalized to the tonic 300 mM NH$_4$Cl response in each animal (as described in the MATERIALS AND METHODS section) and are presented as the mean ± SEM of the relative peak phasic response from three animals.

HCl (r–s) was significantly smaller relative to control (h–i). This treatment affected neither the phasic nor the tonic responses to 0.3 M NH$_4$Cl (unpublished data). This suggests that at this concentration, flufenamic acid most likely does not uncouple gap junctions and does not produce nonspecific effects (Srinivas and Spray, 2003). Thus the effect of flufenamic acid inhibition of the phasic responses is modality specific. The observation that a longer time exposure to flufenamic acid is required to inhibit the membrane conductance suggests that this conductance is most likely localized in the basolateral membrane of TRCs.

Applying a +60 mV transepithelial voltage enhanced the phasic response to HCl and flufenamic acid inhibited the phasic CT response at 0 and +60 mV (Fig. 13 B) relative to control (Fig. 13 A). Peak phasic response to HCl was monitored for a range of voltages between −80 and +80 mV in three animals before and after flufenamic acid treatment. The data demonstrate that the channel becomes activated at positive voltages (Fig. 13 C, ●). Flufenamic acid inhibited the membrane conductance at all applied voltages (Fig. 13 C, ○).

Effect of Chelating TRC [Ca^{2+}]$_i$ with BAPTA on the CT Responses to Acidic Stimuli. Shrinkage-activated flufenamic acid–sensitive cation conductance was reported to be indifferent to changes in [Ca^{2+}]$_i$ (Koch and Korbmacher, 2000). Therefore, if this channel is linked to sour taste transduction, then the phasic CT response to acids should also be indifferent to changes in TRC [Ca^{2+}]$_i$. We loaded TRCs in vivo with BAPTA-AM. BAPTA-AM is membrane permeable, and once inside

the cell, the -AM group is hydrolyzed by intracellular nonspecific esterases, and free acid is released. BAPTA-acid chelates free intracellular Ca^{2+} and decreases resting TRC [Ca^{2+}]$_i$. In addition, any increase in [Ca^{2+}]$_i$ during taste transduction, due either to the release of Ca^{2+} from intracellular stores or the influx of Ca^{2+} through membrane voltage-gated Ca^{2+} channels (VGCCs) in TRC membranes, is buffered by intracellular BAPTA. CT responses to 20 mM HCl were recorded before and after topical lingual application of 30 mM BAPTA-AM. BAPTA completely inhibited the tonic
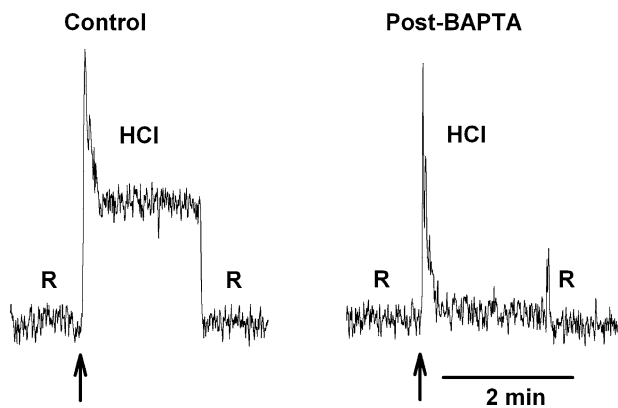
Figure 14. Effect of BAPTA loading on CT response to HCl. The CT responses to 20 mM HCl were recorded relative to the rinse (R = 10 mM KCl) before (Control) and after (Post-BAPTA) treating the tongue with 30 mM BAPTA-AM for 30 min.

phase of the CT response to HCl stimulation (Fig. 14, post-BAPTA) relative to control without affecting the transient phasic response. In three such experiments after BAPTA-AM treatment, the tonic CT response to HCl was not different from baseline. Similar results were obtained with CO_2 and acetic acid stimulation after BAPTA treatment (unpublished data). This indicates that the phasic CT response to acidic stimuli is indifferent to changes in TRC $[Ca^{2+}]_i$ while the tonic phase is sustained by an increase in TRC Ca^{2+}.

DISCUSSION

In this study, we present new evidence that suggests that following a decrease in pH_i, the proximate sour stimulus, the downstream transduction mechanisms for the phasic and tonic components of the CT response to acid stimulation follow distinct and separate pathways. Our results demonstrate a strong relationship between the acid-induced decrease in TRC pH_i, actin cell cytoskeleton, cell shrinkage, flufenamic acid–sensitive membrane cation conductance and the phasic part of the CT response to acidic stimuli. The relationship between pH_i and each of the above events as they relate to the phasic part of the CT response to acid stimulation and to the overall sour taste transduction is discussed below.

Relationship between Osmotically Induced Changes in TRC Volume and pH_i

In many cell types, osmotic changes in cell volume are accompanied by changes in pH_i. Typically, osmotic cell swelling results in a decrease and osmotic shrinkage in an increase in pH_i (Jakab et al., 2002). Consistent with this, osmotic shrinkage of TRCs also resulted in cell alkalinization during RVI, and osmotic swelling produced a decrease in pH_i during RVD (Fig. 1 A). In the nominal absence of HCO_3^-, basolateral NHE-1 serves

as a major pH recovery mechanism in TRCs (Vinnikova et al., 2004). Since both pH_i and cell volume recovery from an intracellular acid load were dependent upon the presence of Na^+ in the basolateral compartment (Fig. 1 D), it suggests that following osmotic shrinkage, both pH_i recovery and RVI are due, in part, to the activation of NHE-1 (Su et al., 2003). However, in the absence of external Na^+, step changes in basolateral NH_4Cl concentration produced a graded decrease in pH_i (Fig. 2 A). At each step, the decrease in pH_i demonstrated a small but significant pH_i recovery. This indicates that besides NHE-1, Na^+-independent pH regulatory mechanisms also operate in TRC membranes and participate in pH_i and cell volume recovery. Osmotic shrinkage is an important activator of the Na^+-H^+ exchanger (Su et al., 2003). The intracellular signaling mechanisms by which shrinkage activates the exchanger have not been fully elucidated. However, it is likely that additional pH regulatory mechanisms, membrane channels and transporters, and shrinkage-activated pathways, such as myosin light chain kinase and other signaling pathways, may also be involved in RVD (Lang et al., 1998; Putney et al., 2002; Wehner et al., 2003).

Relationship between TRC pH_i and Cell Volume

Osmotic cell swelling and shrinkage produce changes in TRC pH_i (Figs. 1–6). However, the notion that at constant pH_o and osmolarity a primary change in pH_i can produce a change in cell volume has only been recognized recently. Fraser et al. (2005) were the first to demonstrate that a primary increase in the acidity of resting frog skeletal muscle cells decreases cell volume. Here we demonstrate that at constant pH_o and osmolarity, a primary change in TRC pH_i modulates cell volume. This relationship was observed irrespective of the method used to produce changes in pH_i. Although the rate of pH_i recovery due to the activation of pH recovery mechanisms from intracellular acidosis or alkalosis was relatively slower than rapid transient changes in pH_i produced by basolateral NH_4Cl, Na-acetate, or CO_2 pulses, even under these conditions, pH_i recovery demonstrated a near linear relationship with TRC volume. These results indicate that cell volume changes occur at the rate at which TRC pH_i is varied.

At present the exact mechanism by which changes in pH_i modulate TRC volume is not known. In the nominal absence of HCO_3^-, changes in pH_i induced by the NH_4Cl pulse produce parallel changes in TRC volume in the absence of external Na^+ (Fig. 1 D and Fig. 2 A). In addition, the relationship between basolateral pH_o, TRC pH_i, and volume was not altered by external K^+ or Cl^- (unpublished data). This suggests that pH_i induces changes in TRC volume independently of Na^+, K^+, Cl^-, or HCO_3^--linked transporters. In contrast, the sponta-

neous pH_i recovery from an intracellular acid or alkaline load involves Na^+, K^+, Cl^-, or HCO_3^--dependent transporters (Putnam et al., 2004). Recent studies suggest that an increase in intracellular H^+ titrates the mean charge (z_x) of the intracellular membrane-impermeant anions (X_i^-) and causes cellular volume decrease (Fraser et al., 2005). This is consistent with the well-known properties of polyelectrolytes in solution. Polyelectrolytes, composed of similarly charged monomers, exist in a volume-expanded state while the corresponding neutralized molecule will encompass a smaller volume (Rice and Nagasawa, 1961). As might be expected by analogy with Donnan potentials, a decrease in the mean charge on the impermeable anion by titration also leads to membrane potential depolarization. Our results suggest that changes in pH_i can also alter cell volume by shifting the equilibrium of F- and G-actin toward G-actin, thus altering cell structure and function. Whether charge titration is also associated with the F- to G-actin transformation is, however, presently unknown.

Regulation of TRC pH_i and Cell Volume by $[Ca^{2+}]_i$

Changes in both pH_i and TRC volume are regulated by $[Ca^{2+}]_i$ through the activation of the basolateral NHE-1 (Fig. 4). Changes in $[Ca^{2+}]_i$ produced similar results in rat alveolar type II cells (Murao et al., 2005). Treating Ehrlich ascites tumor cells with lysophosphatidic acid increased $[Ca^{2+}]_i$ and produced initial cell shrinkage due to the activation of Ca^{2+}-dependnent K^+ and Cl^- efflux, followed by activation of Na^+-H^+ exchanger and RVI, resulting in cell swelling (Pedersen et al., 2000). This suggests that during acid taste transduction, acid-induced increase in TRC $[Ca^{2+}]_i$ (Liu and Simon, 2001; Lyall et al., 2003; Richter et al., 2003) will activate basolateral NHE-1 and facilitate cell volume recovery, resulting in neural adaptation (Lyall et al., 2002a, 2004a).

Relationship between pH_o, TRC pH_i, and Volume

Cell volume changes were also induced by alterations in pH_o (Fig. 2 B and Figs. 3 and 6). Varying the basolateral pH between 7.8 and 6.7 (Fig. 2 B) induced an almost linear change in TRC pH_i with a mean slope of 0.7 (Lyall et al., 2001). Increasing basolateral pH induced intracellular alkalinization and increased cell size. Conversely, a decrease in basolateral pH induced intracellular acidification and decreased cell size. This relationship between pH_i and volume was linear between pH 6.9 and 7.5. Under these conditions no spontaneous pH_i recovery was observed. This is due to the fact that NHE-1 activity is differentially regulated by pH_o and pH_i. At constant pH_o, a decrease in pH_i activates NHE-1. On the contrary, a decrease in basolateral pH_o inhibits NHE-1 (Vinnikova et al., 2004). In the absence of pH_i recovery, spontaneous RVI is not observed (Fig. 1 D). We also did not observe spontaneous pH_i recovery at alkaline basolateral pH. It is likely that the pH regulatory mechanisms involved in lowering alkaline pH_i to baseline are active at the physiological pH (Fig. 1, A and C) but are inhibited at more alkaline basolateral pH. During stimulation of the apical membrane with acid stimuli there was also a direct relationship between a decrease in pH_i and cell volume (Fig. 3). Under these conditions no spontaneous pH_i recovery was also observed. This is due to the inhibition of the basolateral NHE-1. It is suggested that a change in apical pH_o induces inhibition of NHE-1 through changes in the cell cytoskeleton (Lyall et al., 2004a).

Relationship between Cytoskeletal Elements, TRC pH_i, and Volume

Several studies suggest a link between cell cytoskeleton and cell volume. Changes in cellular F-actin content and/or distribution have been reported in cells treated with hypo- or hypertonic solutions (Pedersen et al., 2001; Jorgensen et al., 2003; Ebner et al., 2005). Disruption of F-actin delayed or in some cases totally inhibited volume regulation and Na^+-H^+ exchanger (Linshaw et al., 1991; Ebner et al., 2005). Treatment of fungiform papillae with cytochalasin D diminished the positive reactions in the taste pore cells and increased the inner diameter of the ring reactions (Ohishi et al., 1999). Ethanol transiently shrinks TRCs (Lyall et al., 2005a,b) presumably through modifications of F-actin content (Siegmund et al., 2004). Our data suggest that osmotic effects and changes in cytoskeleton produce additive effects on the phasic CT response to acids (Figs. 5, 9, and 10). The CT responses to mannitol alone, mannitol + acidic stimuli (Fig. 10), and mannitol + NaCl (unpublished data) were attenuated after treating the cell with cytochalasin B or phalloidin. It is suggested that changes in cytoskeletal elements may directly regulate the activity of membrane transporters that are involved in volume and pH regulation (Kurashima et al., 1999; Wehner et al., 2003). In our studies, a decrease in pH_i modified the actin cytoskeleton of TRCs by shifting the equilibrium from F-actin to G-actin (Fig. 5). In TRCs pretreated with cytochalasin B or phalloidin, changes in pH did not produce the shift from F-actin to G-actin (unpublished data). However, treating TRCs with phalloidin or cytochalasin B (Fig. 6) did not alter the magnitude of the pH_o-induced decrease in pH_i but specifically attenuated the pH_i-induced cell shrinkage. This indicates that in TRCs, phalloidin or cytochalasin B decouple the linear relationship between pH_i and cell volume.

Role of pH_i, Actin Cytoskeleton and Cell Volume in the Phasic Part of the CT Response to Acidic Stimuli

Increasing the osmolarity of the rinse solution with mannitol (Figs. 7–9), cellobiose, or ethanol induced cell shrinkage and elicited transient phasic CT re-

sponses (Lyall et al., 1999, 2005a,b). The above osmolytes give a transient phasic CT response because they alter TRC osmotic pressure, which is an affect quite apart from any further interaction they may or may not have with a specific taste receptor. The results suggest that cell shrinkage is an intracellular signal for the phasic part of the CT response to hypertonic stimuli. Cell shrinkage is accompanied by changes in membrane conductance. In the case of NaCl (Fig. 8 A), osmotic cell shrinkage increased the magnitude of both the phasic (g–h) and tonic (i–j) part of the CT response. This is consistent with the observations that cell shrinkage activates apical amiloride-sensitive ENaC, resulting in a greater apical Na$^+$ flux and an enhanced CT response to NaCl (Lyall et al., 1999). In contrast, hypertonic solutions of urea or ethanol, which readily permeate cell membranes, do not alter cell volume or the CT response to NaCl (Lyall et al., 2005a).

In contrast to its effect on the NaCl response, osmotic shrinkage of TRCs in vivo inhibited the phasic CT responses to acidic stimuli without affecting the tonic part of the CT response (Figs. 7 and 9–11). The results suggest that for the phasic response, the downstream intracellular signal after a decrease in pH$_i$ is a decrease in cell volume. The pH$_i$ induces a decrease in cell volume by altering the equilibrium of the actin cytoskeleton from F-actin to G-actin (Fig. 5). This is supported by the observations that the phasic response to acidic stimuli is blocked by osmotic cell shrinkage, cytochalasin B, or phalloidin treatment, and that the osmotic effects are additive with cytochalasin B or phalloidin treatment. While cytochalasin B shifts the equilibrium of the actin cytoskeleton from F-actin to G-actin, phalloidin binds to F-actin and stabilizes the cell cytoskeleton. Therefore, both these treatments tend to attenuate pH$_i$-induced changes in cell volume (Fig. 6). Data shown in Fig. 10 demonstrate that phalloidin can partially reverse the F-actin to G-actin shift. This is demonstrated by the observation that phalloidin partially reversed the inhibition of the phasic response induced by cytochalasin B pretreatment. This is an important observation and strengthens the notion that a decrease in pH$_i$ induces changes in volume through the actin cytoskeleton that modulates the phasic part of the CT response to acids.

Changes in Cytoskeleton and Cell Volume Are Coupled to the Activation of a Flufenamic Acid-sensitive Membrane Conductance

In many cell types, changes in pH$_i$ result in either depolarization or hyperpolarization of the membrane potential (Lyall and Biber, 1994). The changes in potential depend upon the activation or the inhibition of specific membrane conductances. It is likely that changes in the cell cytoskeleton are associated with alterations in TRC membrane permeability. It is suggested that in amphibian skeletal muscle fibers changes in pH$_i$ induce cell shrinkage by altering the activity of intracellular membrane-impermeant osmolytes and the mean charge of the impermeant osmolytes (Fraser et al., 2005). In TRCs containing apical amiloride-sensitive ENaCs, pH$_i$-induced inhibition of the channel will result in hyperpolarization of the apical membrane potential (Lyall et al., 2002b). In cell membranes in which the major membrane conductance is contributed by K$^+$ channels, pH$_i$-induced inhibition of K$^+$ channels will depolarize the potential across the membrane (Lyall et al., 1992). In addition, H$^+$ sensitivity of the leak K$^+$ channel (TASK-2) in TRCs may be an important determinant in setting resting potential and regulating the excitability of TRCs (Lin et al., 2004).

Data summarized in Figs. 11–13 suggest that pH$_i$-induced changes in actin cytoskeleton and the resulting decrease in cell volume activate a membrane conductance. The channel is activated at positive voltages. Examples of such channels include the transient receptor potential (TRP) channels (Nilius et al., 2004; Voets et al., 2004). This channel is most likely a stretch-activated channel since its activity is inhibited by preshrinking cells with hypertonic mannitol (Figs. 11 and 12). Stretch-activated conductance may involve either anion or cation channels. TRCs have been shown to contain stretch-activated Cl$^-$ channels. Their activity is enhanced by osmotic cell swelling and inhibited by NPPB (Gilbertson, 2002). It was reported that in mouse TRCs, acid stimulation activates an NPPB-sensitive Cl$^-$ channel (Miyamoto et al., 1998), suggesting a direct involvement of a Cl$^-$ channel in acid taste transduction. However, in mouse taste cells, NPPB applied to the basolateral side suppressed the citric acid-induced responses but the apically applied NPPB only slightly suppressed the citric acid respond. This suggests that most likely the NPPB-sensitive Cl$^-$ channels are localized in the basolateral membrane (Miyamoto et al., 1998). However, in our studies, topical application of 50 mM NPPB, an inhibitor of swelling activated Cl$^-$ channels, inhibited the phasic part of the CT response to HCl, and the osmotic effects of cell shrinkage were additive with NPPB treatment (DeSimone et al., 2005). At this concentration, NPPB most likely produces nonspecific effects on membrane conductances. This suggests that swelling activated Cl$^-$ channels do not have a significant role during the phasic part of the CT response to HCl stimulation.

Recently, flufenamic acid–sensitive nonselective cation channels activated by cell shrinkage have been described (Koch and Korbmacher, 2000). A flufenamic acid–sensitive cation channel was recently demonstrated in frog taste cell membranes (Sato et al., 2004). The role for NPPB-insensitive poorly selective cation
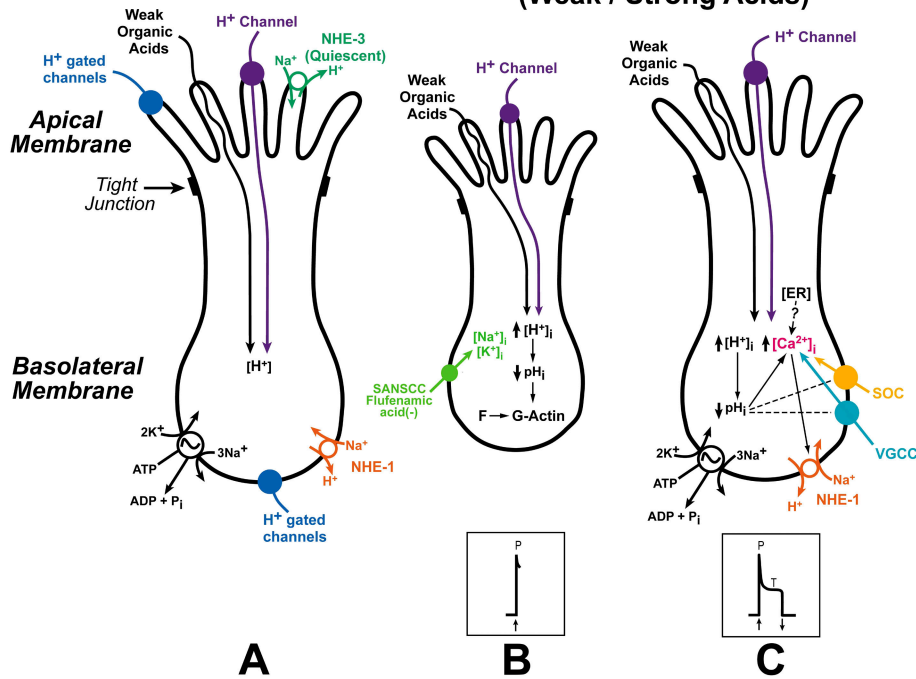
Figure 15. Proposed model for acid transport in fungiform TRCs and sour taste transduction in the anterior tongue. (A) Proposed acid transporters in TRC membranes. (B) An acid-induced decrease in TRC pH$_i$ causes cell shrinkage and the activation of a flufenamic acid–sensitive shrinkage-activated nonselective cation channel that is involved in eliciting the phasic part of the CT response to acidic stimulation (P). (C) In a subset of TRCs a decrease in pH$_i$ induces an increase in [Ca^{2+}]$_i$ that in turn activates basolateral NHE-1. Activation of NHE-1 is responsible for pH$_i$ and cell volume recovery and for the neural adaptation (tonic response [T]) in the CT response to acid stimuli. The abbreviations used in the figure are as follows: H$^+$-gated channels (HCN, hyperpolarization-activated channel; ASIC, acid-sensing ion channel; TASK-2, a two pore domain K$^+$ channel); NHE-1, basolateral Na$^+$-H$^+$ exchanger; NHE-3, apical Na$^+$-H$^+$ exchanger; SANSCC, shrinkage-activated nonselective cation channel; SOC, store-operated Ca^{2+} channel; VGCC, voltage-gated Ca^{2+} channels; activation (+); Inhibition (−); increase (↑); decrease (↓). See text for details.

conductance in mouse taste cells in sour taste transduction has been suggested (Miyamoto et al., 1998). Data summarized in Figs. 12 and 13 strongly support the conclusion that an acid-induced decrease in pH$_i$ decreases TRC volume, resulting in the activation of shrinkage-activated flufenamic acid–sensitive cation channels. The resulting increase in channel conductance is involved in the phasic part of the CT response to acid stimulation. The channel conductance is regulated by the actin cytoskeleton and is inhibited in the presence of hypertonic mannitol. At present, the identity of this putative F-actin– and pH$_i$-induced cell shrinkage–sensitive channel is not known. It has been demonstrated that cell shrinkage activates a nonselective cation channel in a variety of cells. Treating the cells with cytochalasin D inhibited the current response through this nonselective cation channel induced by cell shrinkage (Koch and Korbmacher, 2000). Additional support that this is most likely a cation channel comes from its voltage sensitivity at positive voltages (Figs. 11 and 12). Nonselective cation channels, including TRP channels, demonstrate similar sensitivity at positive voltages (Nilius et al., 2004; Voets et al., 2004). Anion channels have also been described that are regulated by actin cytoskeleton and cell volume (Gilbertson, 2002). However, those channels are activated by cell swelling.

Role of [Ca^{2+}]$_i$ in Acid Taste Transduction

As stated above, following a decrease in pH$_i$, the downstream signaling event in acid taste transduction is an increase in [Ca^{2+}]$_i$ in a subset of TRCs (Liu and Simon, 2001; Lyall et al., 2003; Richter et al., 2003). The increase in [Ca^{2+}]$_i$ and the subsequent activation of basolateral NHE-1 is linked to neural adaptation of CT response to acid stimulation (Lyall et al., 2002a, 2004a). The neural adaptation is related to the tonic part of the CT response to acidic stimuli. Chelating TRC [Ca^{2+}]$_i$ in vivo with BAPTA completely inhibited the tonic phase of the CT response to HCl without affecting the transient phasic part of the CT response (Fig. 14). These results suggest that the transduction events leading to the transient phasic response are indifferent to changes in the Ca^{2+} concentration in the cytosolic compartment of TRCs. We speculate that if an increase in Ca^{2+} concentration in the TRC synaptic regions is required for the initiation of CT nerve activity during the phasic response, these synaptic subregions are not accessible to BAPTA. This would suggest that cytosolic Ca^{2+} and synaptic region Ca^{2+} exist in isolated cell compartments. In this regard it is interesting to note that the flufenamic acid–sensitive shrinkage-activated cation conductance was reported to be insensitive to changes in [Ca^{2+}]$_i$ (Koch and Korbmacher, 2000). This suggests

that the transduction mechanism for the phasic part of the CT response is quite distinct from the tonic part of the neural response to acid stimulation.

The main conclusions of the paper and the proposed mechanisms for the phasic and the tonic CT response to acidic stimuli are summarized in Fig. 15. Fig. 15 A shows the proposed acid transporters in TRC membranes. Acid equivalents enter TRCs across the apical membrane by at least two mechanisms and decrease pH_i. For fully dissociated strong acids, H^+ ions permeate the apical membrane through an amiloride- and Ca^{2+}-insensitive, but cAMP-sensitive pathway (Lyall et al., 2002a). Weak acids on the other hand cross the apical membrane as neutral molecules and generate intracellular acid equivalents. At present it is not clear if H^+-gated channels (ASIC, HCN, and TASK-2 K^+ channels) also play a role in sour taste transduction (Ugawa et al., 1998; Stevens et al., 2001; Lin et al., 2002; Richter et al., 2004b). In Fig. 15 B, an acid-induced decrease in pH_i in a subset of TRCs alters the cell cytoskeleton by shifting the F- to G-actin equilibrium toward G-actin and by titrating the mean charge of the intracellular membrane-impermeant anions, which could include elements of the cytoskeleton (Fraser et al., 2005), resulting in cell shrinkage. The pH_i-induced decrease in cell volume activates a flufenamic acid–sensitive shrinkage-activated nonselective cation channel (SANSCC) in the basolateral membrane of TRCs. The entry of one or more monovalent cations through SANSCC depolarizes the receptor potential and is the basis for the phasic (P) component of the CT response to acidic stimuli. The phasic part of the CT response to acids seems to be indifferent to changes in cytosolic Ca^{2+} should they occur during this phase. Fig. 15 C shows that in acid-sensing TRCs, the decrease in pH_i and cell depolarization activate voltage-gated Ca^{2+} channels (VGCCs) or the capacitative Ca^{2+} entry through store-operated Ca^{2+} channels (SOCs) (Pérez et al., 2003), resulting in an increase in TRC $[Ca^{2+}]_i$. Increase in $[Ca^{2+}]_i$, in turn, activates basolateral NHE-1, which is responsible for pH_i and cell volume recovery and for the neural adaptation (tonic response [T]) in the CT response to acid stimuli. The accompanying Na^+ ions exit TRCs across the basolateral membrane via the ouabain-sensitive Na^+-K^+-ATPase. Although NHE-3 is present in the apical membrane of TRCs, under the experimental conditions examined so far, it is quiescent and does not participate in pH_i regulation (Vinnikova et al., 2004).

REFERENCES

Beauchamp, G.K., B. Cowart, and H.J. Schmidt. 1991. Development of chemosensitivity and preference. *In* Smell and Taste in Health and Disease. T.V. Getchell, R.L. Doty, L.M. Bartoshuk, and J.B. Snow, editors. Raven Press, New York. 405–416.

DeSimone, J.A., S. Mummalaneni, T.-H.T. Phan, H. Pasley, G.L. Heck, and V. Lyall. 2005. Effect of pH and cell volume on the phasic chorda tympani response to acid stimulation. *Chem. Senses (Abstr.).* In press.

Ebner, H.L., A. Cordas, D.E. Pafundo, P.J. Schwarzbaum, B. Pelster, and G. Krumschnabel. 2005. The importance of cytoskeletal elements in volume regulatory responses of trout hepatocytes. *Am. J. Physiol. Regul. Integr. Comp. Physiol.* 289:R877–R890.

Fraser, J.A., C.E. Middlebrook, J.A. Usher-Smith, C.J. Schwiening, and C.L. Huang. 2005. The effect of intracellular acidification on the relationship between cell volume and membrane potential in amphibian skeletal muscle. *J. Physiol.* 563:745–764.

Gilbertson, T.A. 2002. Hypoosmotic stimuli activate a chloride conductance in rat taste cells. *Chem. Senses.* 27:383–394.

Hofer, D., and D. Drenckhahn. 1999. Localization of actin, villin, fimbrin, ezrin and ankyrin in rat taste receptor cells. *Histochem. Cell Biol.* 112:79–86.

Jakab, M., J. Furst, M. Gschwentner, G. Botta, M.L. Garavaglia, C. Bazzini, S. Rodighiero, G. Meyer, S. Eichmueller, E. Woll, et al. 2002. Mechanisms sensing and modulating signals arising from cell swelling. *Cell. Physiol. Biochem.* 12:235–258.

Jorgensen, N.K., S.F. Pedersen, H.B. Rasmussen, M. Grunnet, D.A. Klaerke, and S.P. Olesen. 2003. Cell swelling activates cloned Ca^{2+}-activated K^+ channels: a role for the F-actin cytoskeleton. *Biochim. Biophys. Acta.* 1615:115–125.

Koch, J.P., and C. Korbmacher. 1999. Osmotic shrinkage activates nonselective cation (NSC) channels in various cell types. *J. Membr. Biol.* 168:131–139.

Koch, J., and C. Korbmacher. 2000. Mechanism of shrinkage activation of nonselective cation channels in M-1 mouse cortical collecting duct cells. *J. Membr. Biol.* 177:231–242.

Kurashima, K., S. D'Souza, K. Szaszi, R. Ramjeesingh, J. Orlowski, and S. Grienstein. 1999. The apical Na^+-H^+ exchanger isoform NHE3 is regulated by the actin cytoskeleton. *J. Biol. Chem.* 274: 29843–29849.

Lang, F., G.L. Busch, M. Ritter, H. Volkl, S. Waldegger, E. Gulbins, and D. Haussinger. 1998. Functional significance of cell volume regulatory mechanisms. *Physiol. Rev.* 78:247–306.

Lin, W., T. Ogura, and S.C. Kinnamon. 2002. Acid-activated cation currents in rat vallate taste receptor cells. *J. Neurophysiol.* 88:133–141.

Lin, W., C.A. Burks, D.R. Hansen, S.C. Kinnamon, and T.A. Gilbertson. 2004. Taste receptor cells express pH-sensitive leak K^+ channels. *J. Neurophysiol.* 92:2909–2919.

Linshaw, M.A., T.J. Macalister, L.W. Welling, C.A. Bauman, G.Z. Hebert, G.P. Downey, E.W. Koo, and A.I. Gotlieb. 1991. Role of cytoskeleton in isotonic cell volume control of rabbit proximal tubules. *Am. J. Physiol.* 261:F60–F69.

Liu, L., and S.A. Simon. 2001. Acidic stimuli activates two distinct pathways in taste receptor cells from rat fungiform papillae. *Brain Res.* 923:58–70.

Lyall, V., and T.U.L. Biber. 1994. Potential-induced changes in intracellular pH. *Am. J. Physiol.* 266:F685–F696.

Lyall, V., T.S. Belcher, and T.U.L. Biber. 1992. Effect of changes in

extracellular potassium on intracellular pH in principal cells of frog skin. *Am. J. Physiol.* 263:F722–F730.

Lyall, V., G.L. Heck, J.A. DeSimone, and G.M. Feldman. 1999. Effects of osmolarity on taste receptor cell size and function. *Am. J. Physiol.* 277:C800–C813.

Lyall, V., R.I. Alam, D.Q. Phan, G.L. Ereso, T.-H.T. Phan, S.A. Malik, M.H. Montrose, S. Chu, G.L. Heck, G.M. Feldman, and J.A. DeSimone. 2001. Decrease in rat taste receptor cell intracellular pH is the proximate stimulus in sour taste transduction. *Am. J. Physiol. Cell Physiol.* 281:C1005–C1013.

Lyall, V., R.I. Alam, T.-H.T. Phan, D.Q. Phan, G.L. Heck, and J.A. DeSimone. 2002a. Excitation and adaptation in the detection of hydrogen ions by taste receptor cells: a role for cAMP and Ca^{2+}. *J. Neurophysiol.* 87:399–408.

Lyall, V., R.I. Alam, T.-H.T. Phan, O.F. Russell, S.A. Malik, G.L. Heck, and J.A. DeSimone. 2002b. Modulation of rat chorda tympani NaCl responses and intracellular Na^+ activity in polarized taste receptor cells by pH. *J. Gen. Physiol.* 120:793–815.

Lyall, V., S.A. Malik, R.I. Alam, G.L. Heck, and J.A. DeSimone. 2003. Relationship between intracellular pH (pH_i) and Ca^{2+} $[Ca^{2+}]_i$ in fungiform (FF) rat taste receptor cells (TRCs). *Chem. Senses.* 28:A83 (Abstr.).

Lyall, V., R.I. Alam, S.A. Malik, T.-H.T. Phan, A.K. Vinnikova, G.L. Heck, and J.A. DeSimone. 2004a. Basolateral Na^+-H^+ exchanger-1 in rat taste receptor cells is involved in neural adaptation to acidic stimuli. *J. Physiol.* 556:159–173.

Lyall, V., G.L. Heck, A.K. Vinnikova, S. Ghosh, T-H.T. Phan, R.I. Alam, O.F. Russell, S.A. Malik, J.W. Bigbee, and J.A. DeSimone. 2004b. The mammalian amiloride-insensitive non-specific salt taste receptor is a vanilloid receptor-1 variant. *J. Physiol.* 558:147–159.

Lyall V., Heck, G.L., Phan, T-H T., Mummalaneni, S.A. Malik, A.K. Vinnikova, and J.A. DeSimone. 2005a. Ethanol modulates the VR-1 variant amiloride-insensitive salt taste receptor. I. Effect on TRC volume and Na^+ flux. *J. Gen. Physiol.* 125:569–585.

Lyall V., Heck, G.L., Phan, T-H T., Mummalaneni, S.A. Malik, A.K. Vinnikova, and J.A. DeSimone. 2005b. Ethanol modulates the VR-1 variant amiloride-insensitive salt taste receptor. II. Effect on chorda tympani salt responses. *J. Gen. Physiol.* 125:587–600.

Miyamoto, T., R. Fujiyama, Y. Okada, and T. Sato. 1998. Sour transduction involves activation of NPPB-sensitive conductance in mouse taste cells. *J. Neurophysiol.* 80:1852–1859.

Muallem, S., B.X. Zhang, P.A. Loessberg, and R.A. Star. 1992. Simultaneous recording of cell volume changes and intracellular pH or Ca^{2+} concentration in single osteosarcoma cells UMR-106-01. *J. Biol. Chem.* 267:17658–17664.

Murao, H., A. Shimizu, K. Hosoi, A. Iwagaki, K.Y. Min, G. Kishima, T. Hanafusa, T. Kubota, M. Kato, H. Yoshida, and T. Nakahari. 2005. Cell shrinkage evoked by Ca^{2+}-free solution in rat alveolar type II cells: Ca^{2+} regulation of Na^+-H^+ exchanger. *Exp. Physiol.* 90:203–213.

Nilius, B., J. Vriens, J. Prenen, G. Droogmans, and T. Voets. 2004. TRPV4 calcium entry channel: a paradigm for gating diversity. *Am. J. Physiol. Cell Physiol.* 286:C195–C205.

Ohishi, Y., Y. Shiba, C. Hirono, and S. Komiyama. 1999. Effects of cytochalasin D on taste pores of rat fungiform papillae. *Eur. Arch. Otorhinolaryngol.* 256:S38–S41.

Pedersen, S., E.K. Hoffmann, C. Hougaard, and I.H. Lambert. 2000. Cell shrinkage is essential in lysophosphatidic acid signaling in Ehrlich ascites tumor cells. *J. Membr. Biol.* 173:19–29.

Pedersen, S.F., E.K. Hoffmann, and J.W. Mills. 2001. The cytoskeleton and cell volume regulation. *Comp. Biochem. Physiol. A Mol. Integr. Physiol.* 130:385–399.

Pérez, C.A., R.F. Margolskee, S.C. Kinnamon, and T. Ogura. 2003. Making sense with TRP channels: store-operated calcium entry and the ion channel Trpm5 in taste receptor cells. *Cell Calcium.* 33:541–549.

Putnam, R.W., J.A. Filosa, and N.A. Ritucci. 2004. Cellular mechanisms involved in CO_2 and acid signaling in chemosensitive neurons. *Am. J. Physiol. Cell Physiol.* 287:C1493–C1526.

Putney, L.K., S.P. Denker, and D.L. Barber. 2002. The changing face of the Na^+/H^+ exchanger, NHE1: structure, regulation, and cellular actions. *Annu. Rev. Pharmacol. Toxicol.* 42:527–552.

Rice, S.A., and M. Nagasawa. 1961. Polyelectrolyte Solutions. Academic Press, New York. 497–516.

Richter, T.A., A. Caicedo, and S.D. Roper. 2003. Sour taste stimuli evoke Ca^{2+} and pH responses in mouse taste cells. *J. Physiol.* 547: 475–483.

Richter, T.A., G.A. Dvoryanchikov, N. Chaudhari, and S.D. Roper. 2004a. Acid-sensitive two-pore domain potassium (K_2P) channels in mouse taste buds. *J. Neurophysiol.* 92:1928–1936.

Richter, T.A., G.A. Dvoryanchikov, S.D. Roper, and N. Chaudhari. 2004b. Acid-sensing ion channel-2 is not necessary for sour taste in mice. *J. Neurosci.* 24:4088–4091.

Sato, T., Y. Okada, and K. Toda. 2004. Analysis of slow hyperpolarizing potentials in frog taste cells induced by glossopharyngeal nerve stimulation. *Chem. Senses.* 29:651–657.

Scott, T.R., and C.R. Plata-Salaman. 1991. Coding of taste quality. *In* Smell and Taste in Health and Disease. T.V. Getchell, R.L. Doty, L.M. Bartoshuk, and J.B. Snow, editors. Raven Press, New York. 345–368.

Sekerkova, G., L. Zheng, P.A. Loomis, B. Changyaleket, D.S. Whitlon, E. Mugnaini, and J.R. Bartles. 2004. Espins are multifunctional actin cytoskeletal regulatory proteins in the microvilli of chemosensory and mechanosensory cells. *J. Neurosci.* 24:5445–5456.

Siegmund, E., F. Luthen, J. Kunert, and H. Weber. 2004. Ethanol modifies the actin cytoskeleton in rat pancreatic acinar cells-comparison with effects of CCK. *Pancreatol.* 4:12–21.

Srinivas, M., and D.C. Spray. 2003. Closure of gap junction channels by arylaminobenzoates. *Mol. Pharmacol.* 63:1389–1397.

Stevens, D.R., R. Seifert, B. Bufe, F. Muller, E. Kremmer, R. Gauss, W. Meyerhof, U.B. Kaupp, and B. Lindemann. 2001. Hyperpolarization-activated channels HCN1 and HCN4 mediate responses to sour stimuli. *Nature.* 413:631–635.

Su, X., T. Pang, S. Wakabayashi, and M. Shigekawa. 2003. Evidence for involvement of the putative first extracellular loop in differential volume sensitivity of the Na^+/H^+ exchangers NHE1 and NHE2. *Biochemistry.* 42:1086–1094.

Ugawa, S., Y. Minami, W. Guo, Y. Saishin, K. Takatsuji, T. Yamamoto, M. Tohyama, and S. Shimada. 1998. Receptor that leaves a sour taste in the mouth. *Nature.* 395:555–556.

Vinnikova, A.K., R.I. Alam, S.A. Malik, G.L. Ereso, G.M. Feldman, J.M. McCarty, M.A. Knepper, G.L. Heck, J.A. DeSimone, and V. Lyall. 2004. Na^+-H^+ exchange activity in taste receptor cells. *J. Neurophysiol.* 91:1297–1313.

Voets, T., G. Droogmans, U. Wissenbach, A. Janssens, V. Flockerzi, and B. Nilius. 2004. The principal of temperature-dependent gating in cold- and heat-sensitive TRP channels. *Nature.* 430:748–754.

Wehner, F., H. Olsen, H. Tinel, E. Kinne-Saffran, and R.K. Kinne. 2003. Cell volume regulation: osmolytes, osmolyte transport, and signal transduction. *Rev. Physiol. Biochem. Pharmacol.* 148:1–80.